博士論文

(Doctoral Thesis)

Study on the effects of Diindolylmethane on autophagy and apoptosis in fission yeast

ジインドリルメタンの分裂酵母オートファジーやアポトーシスへの効果の研究

Parvaneh Emami

広島大学院統合生命科学研究科

Graduate School of Integrated Sciences for Life

Hiroshima University

2022年8月

August 2022

Contents

Chapter1. Introduction 2

1.1. Fission yeast, a eukaryotic model organism 2

1.1.1. Apoptosis in fission yeast 4

1.1.2. Autophagy in fission yeast 6

1.2. DIM and apoptosis 9

1.3. DIM and autophagy 10

1.4. Aim of the thesis 12

Chapter 2. 3,3'-Diindolylmethane (DIM) is suggested to induce apoptosis and causes autophagy in fission yeast 15

2.1. Introduction 15

2.2. Material and method 18

2.2.1. Strains construction 19

2.2.2. Viability assay by spot test 21

2.2.3. Acute viability assay by spot test 22

2.2.4. Quantitation of the percentage of viability 22

2.2.5. Apoptosis detection by acridine orange/ethidium bromide (AO/EB) and 4',6-diamidino -2-phenylindole 23

2.2.6. Microscopy 24

2.2.7. ATP level measurement 25

2.2.6. Nitrogen starvation and the condition in which DIM induces autophagy 27

2.2.7. Viability assay by spot test in DIM autophagy inducing condition 27

2.2.8. Statistical analysis 28
2.3. Results and discussion 29
2.3.1. DIM reduces cell viability in log-phase cells, but not in stationary-phase cells 29
2.3.2. Acute effect of DIM on log-phase and stationary-phase cells 32
2.3.3. DIM is suggested to induce apoptosis in log-phase cells.....34
2.3.4. DIM induces nuclear condensation and NE disruption in log-phase cells within ten minutes. 38
2.3.5. Mitochondrial ATPase may not be the first target of DIM in fission yeast. 41
2.3.6. Autophagy is induced by DIM, and the autophagy pathway but not the ER stress response pathway is required for the resistance to DIM 43
2.3.7. Nuclear membrane protein, Lem2, is required for the resistance to DIM 50
2.4. Summary 55
Chapter 3. Conclusion 59
3.1. Thesis summary 59
3.2. Achievements of the thesis and more discussion 63
3.3. Future perspectives 65
Media Appendix 68
Protocol Appendix 71
References 80
Acknowledgment 94

Organization of this thesis

Chapter 1 contains some background information about apoptosis and autophagy. In continue, DIM will be introduced and its potential role in cancer therapy, the known direct targets, and the possible mechanism in apoptosis or autophagy will be mentioned. Finally, a brief introduction of fission yeast as a eukaryotic model organism, and the aims of this thesis will be explained.

Chapter 2 will be started with a brief introduction to DIM and then describes my study of "**3,3'-Diindolylmethane (DIM) is suggested to induce apoptosis and causes autophagy in fission yeast**", to show how I demonstrated the apoptotic and autophagic effects of DIM on fission yeast for the first time, and finding the nuclear envelope (NE) as one of the early targets for DIM in fission yeast in vivo condition. I also explain the role of Lem2, an inner nuclear protein, and autophagy pathway for DIM tolerance in a low concentration.

Chapter 3 is a conclusion for all of the results and some ideas for future experiments.

Chapter 1

Introduction

Chapter1. Introduction

1.1. Fission yeast, a eukaryotic model organism

Schizosaccharomyces pombe (*S. pombe*) is a species of "fission yeast". It is a unicellular eukaryote organism in a rod shape. Normally, fission yeast cells have 3 to 4 micrometers in diameter and 7 to 14 micrometers in length and contain about 14.1 million base pairs genomic information. Fission yeast has been used as a laboratory organism since the 1950s [1]. Its genome has been fully sequenced as the sixth model eukaryotic organism, following the budding yeast, *Caenorhabditis elegans*, *Drosophila melanogaster*, *Arabidopsis thaliana* and the human [2]. It belongs to ascomycete fungi group. Fission yeast genome is organized in three chromosomes. Predominantly, fission yeast exists with one set of chromosomes (haploid), which is easily propagated and used for screening the mutants and experiments. Diploid cells have a longer size which are used to determine the recessive or dominant status of alleles.

Such as every eukaryotic cell, vegetative cells of fission yeast, have a mitotic cycle. Its mitotic cycle includes S-phase (Synthetic phase), which will be followed by nuclear division (mitosis) and cell division (cytokinesis) (Fig. 1.1A). There is a G1 phase (gap 1) between M and S phases. G2 (gap 2) is a middle phase between S and M phases [3]. G1, S, and G2 are collectively named interphase. Growth of yeast has different phases, containing lag-phase with lag in growing, log-phase with fast-

growing and high cell division, and stationary-phase without cell division and no growth (Fig. 1.1B).

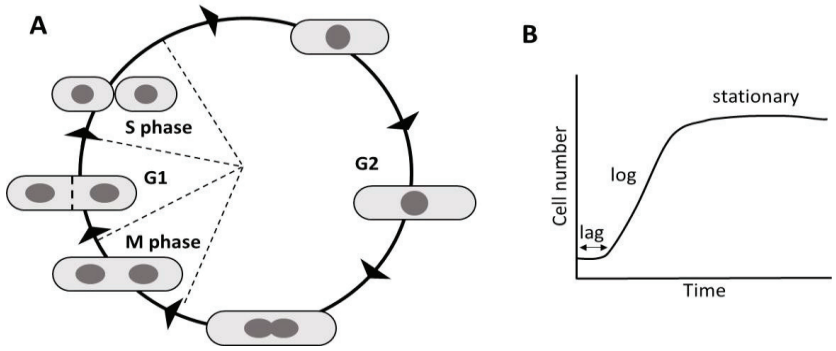

Fig 1.1. Cell phase (A) and growth phase (B) of haploid cells in fission yeast.

In contrast to human cells, fission yeast cells undergo the "closed mitosis" while the intact nuclear envelope (NE) is kept during mitosis [4].The rate of cell division in vegetative growth is related to the nutrients and temperature and may need 2 to 4hrs for one cell division [1]. Usually, after one day growing in yeast extract medium, growth phase of log-phase cells reaches stationary-phase. Growing fission yeast is inexpensive. Its genome could be manipulated easily. Fission yeast has some similarities to humans [5], including chromatin dynamics, gene structures, the control of gene expression through pre-mRNA splicing, epigenetic gene silencing, and RNAi pathways [6]. Its life cycle and aspects of its biology make fission yeast a useful model organism for study of eukaryotic molecular and cell

biology [1] and the mechanism of pathways such as apoptosis [7-10] and autophagy [11, 12].

1.1.1. Apoptosis in fission yeast

Apoptosis is a process that results in the death of damaged and unrepairable cells to maintain health in multicellular organisms [13]. It also happens in fission yeast and can be characterized by morphological features such as chromatin breakage, nuclear fragmentation [14, 15], NE disruption [16] and cell death [10, 14, 17] in fission yeast (Fig. 1.2).

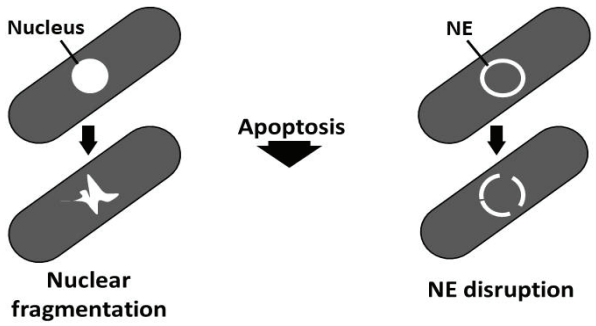

Fig 1.2. Apoptosis morphological feature in fission yeast. Apoptosis induction is detectable by nuclear fragmentation and NE disruption in fission yeast cells**.**

Apoptosis could be induced by different conditions in fission yeast such as pH stress [10] . It could be also induced through the oxidative stress pathway by some compounds such as terpinolene, an odorant in the cosmetics industry [14], or alpha-thujone, which is a compound in the food industry [7]. Camphor, a pharmaceutical compound, is another apoptotic cell death inducer in *sod1Δ* fission

yeast cells, which have defects to scavenge free radicals in the cell [18]. Starvation of inositol, which is a precursor of numerous phospholipids and involved in signaling pathways, induces apoptosis through the ER stress induction in fission yeast [15]. Gene expression could be also involved in apoptosis induction. Overexpression of endogenous gene such as *calnexin* in fission yeast causes apoptotic cell death, which partially depends on the Ire1, the ER-stress transducer [17]. On the contrary, *dga1Δplh1Δ* double mutant, which is defective in lipid metabolic pathway, promotes apoptosis in fission yeast [19, 20]. The expression of heterologous genes such as *bax* and *bak* from human also promotes apoptosis in fission yeast [21]. Both Bax and Bak belong to the Bcl-2 family proteins which control apoptosis by governing mitochondrial outer membrane permeabilization [22]. The ectopic expression of mitochondria endonuclease of fission yeast, *pnu1* (homolog of EndoG in human), also leads to nuclear fragmentation and apoptosis in fission yeast [23].

Not only the pathways and type of the stimulator are different for apoptosis induction in fission yeast, but also, studies show that apoptotic cell death happens in different cell phases, and in some cases, stationary-phase cells are more sensitive to apoptotic inducing conditions or vice versa, apoptosis happens more in the log-phase cells. Deletion of *dga1* and *plh1* in fission yeast cells only triggers apoptosis when cells enter stationary-phase [20]. Apoptosis also happens in stationary-phase cells when cells are exposed to inositol starvation [15] or valproic acid [10] or when

calnexin is overexpressed [17]. In contrast, some studies show apoptosis induction in log-phase cells when camphor [18], alpha-thujone [7] are used. This information implies that the study of apoptosis mechanism in different growth phases of fission yeast is important.

1.1.2. Autophagy in fission yeast

Autophagy recycles the cellular components such as damaged proteins or organelles [24, 25]. It can be induced by stress or nutrient starvation in fission yeast [26]. The damaged proteins, organelles or cytoplasmic compounds which called cargo, will be sequestrated within membranes called autophagosomes. Finally, after fusing the autophagosome with the vacuole, cargo will be degraded in vacuole of fission yeast [26] (Fig. 1.3).

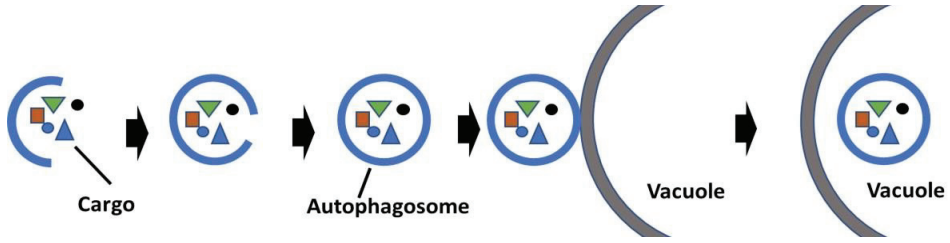

Fig 1.3. Autophagy process in fission yeast. By autophagy induction, cytoplasmic cargo will be sequestrated within autophagosomes and subsequently fused with the vacuole in fission yeast cells. Finally, cargo will be degraded in the vacuole.

There are selective and non-selective autophagy pathways in fission yeast [27]. In non-selective autophagy (bulk autophagy), bulk portions of the cytoplasm are sequestered and form autophagosomes. Non-selective autophagy happens to maintain the nutrient levels in starved cells or intracellular homeostasis in non-starved cells [28] In contrast, in selective autophagy, specific cargo based on the specific receptor will be selected for autophagy process [28].

More than 40 autophagy-related proteins have been identified in budding yeast [29]. However, about 23 autophagy-related proteins have been detected in fission yeast [30] and Atg8 is one of them. Atg8 is critical for autophagosome formation in fission yeasts [12, 31] which is used as a general autophagy marker. Atg8 is distributed in the cytoplasm but forms bright foci when autophagy is induced by nitrogen starvation if it was tagged by fluorescent proteins [26, 30, 32].

Autophagy can be induced in fission yeasts via different conditions [30, 33]. Entry into the stationary-phase induces autophagy in fission yeast to recycle the nutrients [34] or detoxify of some poisoning compounds such calnexin in cells [35]. Nitrogen starvation induces autophagy in fission yeast to generate a nitrogen source for adaptation [26, 34]. Sulfur starvation also induces autophagy in fission yeasts which is controlled by *ecl1* family genes [36] and autophagy contributes to maintaining cellular viability in both nitrogen [11] and sulfur starvation [36]. ER stress is also involved in autophagy induction by Dithiothreitol (DTT) [33]. On the other side, autophagy can be induced by TORC1 inhibition in fission yeast [37].

However, in contrast to the budding yeast, rapamycin, the inhibitor of TORC1 in fission yeast, does not induce autophagy in this species of yeast [26], which shows the complexity of autophagy process.

1.2. DIM and apoptosis

3,3'-Diindolylmethane (DIM) is a compound derived from the digestion of indole-3-carbinol, found in the plants from the broccoli family, such as cabbage, broccoli, and rape [38]. Recent studies reported that DIM has anticancer effects through the induction of apoptotic cell death in breast cancer [39, 40], hepatoma [41, 42], prostate cancer [43, 44], or colon cancer [45-47]. Apoptosis is a promising target for cancer therapy because it induces cell death in cancer cells, therefore DIM ability to induce apoptosis makes it a potential anti-cancer drug for future studies in human biomedical science.

Studies showed the different pathways for DIM to induce apoptosis, such as bax- and p53-independent pathways in MCF-7 breast cancer cells [48]. Another study about the effects of DIM on prostate cancer resulted to find the mitochondrial pathway as an apoptosis induction [43, 49]. It is assumed that the release of calcium from ER into the cytosol is another mechanism of DIM to induce apoptotic in prostate cancer, cervical cancer [50], and gastric cancer [51]. The generation of ROS is the next possible pathway to induce apoptosis in breast cancer cells by DIM [39]. In contrast, DIM can inhibit apoptosis and reduces ROS and oxidative stress in H9c2 myoblasts [52] or neuronal cells [53]. These were some of the mixed and contradictory information about the effects of DIM on apoptosis induction which show the direct mechanism of DIM to trigger apoptosis is still unknown.

Even direct target(s) of DIM in vivo condition still is unknown. However, the results of the study showed that DIM inhibits mitochondrial F1F0-ATPase [54] in MCF-7 breast cancer cells. DIM also reduces ATP level and arrest the MCF-7 cells [55]. A recent report showed that DIM inhibits the activity of Cox1/2, a prostaglandin synthase, in vitro condition, and it suppresses the growth of colon cancer cells [47]. The study of DIM effects in MCF-7 breast cancer cells showed a rapid accumulation of DIM in their nuclear membranes (NM, a part of NE) after 0.5–2 hours [56]. The outcome of the accumulation of DIM in NM remains unclear. The similarity of fission yeast and human biological pathways helps to study the DIM apoptotic mechanism. Here the role of DIM in apoptosis induction in fission yeast cells was studied. Moreover, the investigation of DIM effects on NE in fission yeast was selected as a part of this study.

1.3. DIM and autophagy

As mentioned autophagy recycles the cellular components such as damaged proteins or organelles to keep cells save or kill them. In one way, upregulation of autophagy extends the lifespan of the animal [57]. Autophagy by recycling nutrients or degradation of damaged proteins, protects the cell, and promotes cell survival [58, 59] which could be undesirable in cancer therapy. On the other way, it is believed that autophagy is a device to process a type of cell death, which is called autophagic cell death, ACD [60]. Some human results showed that autophagy induction can

suppress the growth of cancer cells [31, 61-63]. Therefore, autophagy has several potential benefits for human health, including life longevity and cancer therapy due to its double-edged sword of autophagy function.

Studies showed that DIM also has the potential role in regulating autophagy. However, the studies indicate the role of DIM to induce or inhibit autophagy in various pathways. DIM inhibits the proliferation of gastric cancer cells through the autophagy induction mediated by microRNA [63]. In ovarian cancer cells, DIM increases the cytosolic calcium to regulate AMPK pathway and autophagy which suppress cancer cells [61]. DIM also induces autophagy in them through the endoplasmic reticulum (ER) stress induction [61]. In ovarian cancer, DIM increases *ire1* expression and subsequently induces autophagy, and inhibits the growth of the tumors. Inhibition of ER stress and subsequently prevent from ER stress response (unfolded protein response, UPR) suppresses autophagy induction, which suggests that the ER stress response excites the autophagy induction by DIM.

It is known that DIM induces ER stress and autophagy in prostate cancer cells [64]. However, mitochondrial dysfunction is a reason that DIM kills prostate cancer cells, not ER stress induction or autophagy. In fact, autophagy induced by DIM is for protecting the prostate cancer cells not for suppressing them [64]. Similarly, it was reported that autophagy induction by DIM in H9c2 myoblasts cells suppresses apoptosis and hypoxia through the superoxide dismutase (sod) pathways and saves the myoblasts cells [52], instead of killing them.

Even, some results showed the other aspect of DIM to inhibit the autophagy. For example, DIM has a protective role against ischemia in neuronal cells by inhibition of the autophagy and apoptosis [65]. It seems that the mechanism of the DIM to induce or inhibit the autophagy is still unclear. It is also unknown that autophagy induced by DIM suppresses cancer cell or protects them. These results show the importance of further studies in this case. Here, I showed DIM induces autophagy when it is in low concentration. In addition, I found that autophagy has a protective role to save the cells when DIM is used.

1.4. Aim of the thesis

Targeting apoptosis is one the efficient and useful methods in cancer therapy. Cancer cells tend to inhibit apoptosis to survive. Autophagy may also behave as an anti-aging process, or in contrast, act as a mechanism to suppress or kill the cancer cells in different conditions. Finding the new types of anti-cancer drugs is one aim of human health sciences to cure cancer cells. DIM is one of the promising anti-cancer drugs however, the mechanism of DIM to induce apoptosis or autophagy in human is not fully understood.

In another way, a drug may have different targets and affect the multi pathway, therefore using a big and complicated genome of human, makes the studies harder. The autophagy and apoptosis pathways might be conserved in fission yeast and humans. Using fission yeast as a simple eukaryotic model makes the study

simpler, faster, and more efficient. Thus, I performed my experiments on fission yeast to understand:

Does DIM induce apoptosis in fission yeast? If yes what is the earliest event(s) in apoptosis induction?

Does DIM induce autophagy in fission yeast? If yes what is the possible mechanism to induce autophagy by DIM?

Is there any direct target(s) of DIM in vivo condition?

In the next chapter, I will explain my results to show how I found “DIM is suggested to induce apoptosis and causes autophagy in fission yeast”.

Chapter 2

3,3’-Diindolylmethane (DIM) is suggested to induce apoptosis and causes autophagy in fission yeast

Chapter 2. 3,3'-Diindolylmethane (DIM) is suggested to induce apoptosis and causes autophagy in fission yeast

2.1. Introduction

The nucleus of yeast cells is surrounded by a nuclear envelope (NE). NE contains an inner nuclear membrane (INM), an outer nuclear membrane (ONM), and nuclear pore complexes (NPCs) [66]. NE keeps the genomic content far from harmful cytoplasmic components such as cytosolic nucleases. Homeostasis of NE is maintained by lipid metabolic enzymes [67]. One of the required NE proteins that has a big role in homeostasis of NE [67, 68], is Lem2 which is an inner nuclear protein. Lem2 acts as a barrier for membrane flow between the nucleus and ER [69], and the cells without Lem2, are more sensitive to the condition that fatty acid synthesis is inhibited [69]. The quantity of C24:0 fatty acid is reduced in *lem2*Δ*bqt4*Δ mutant and affects membrane integrity [67]. However, the deletion of *lem2* itself, leads to nuclear protein leakage slightly [67].

Lem2 with Lnp1 (an ER protein) are cooperatively involved in the maintenance of the boundary between NE and ER membrane [70]. The distribution of NE protein, Ish1, is also affected in *lem2Δlnp1Δ* [70], which leads to abnormal NE morphology and severe nuclear protein leakage in almost all cells and reduces the cell viability when *lem2* and *lnp1* are deleted [70].

Moreover, in fission yeast, ESCRT-III complex (endosomal sorting complex required for transport-III) and Vps4 (AAA-ATPase) make a part of ESCRT machinery to repair the nuclear envelopes [68, 71]. (Fig. 2.1). To repair the NE, ESCRT-III needs Cmp7, a multivesicular body, and to complete the process of sealing, Vps4 disassembles ESCRT-III [68]. Since the deletion of *lem2 r*educes the protein amount of Vps4 in cell and defuses the localization of Cmp7 [70], It is possible that Lem2 may have a potential role in the sealing process of NE by ESCRT-III. Without proper sealing of NE, the nucleus may be easily affected by cytosolic compounds and get damaged, therefore, the possible cell death may be triggered.

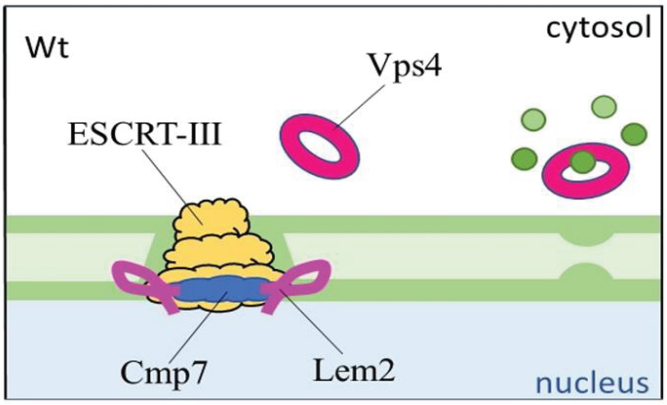

Fig 2.1. ESCRT-III machinery is responsible to seal the NE. Lem2 recruits Cmp7 for ESCRT-III to seal NE and Vps4, which is AAA family ATPase, will disassemble ESCRT-III to finish the sealing process.

As explained in chapter 1, 3,3'-Diindolylmethane (DIM) is one of the potential apoptosis inducers in human cells [39, 40, 42, 43]. On the other hand, DIM

induces autophagy in human cells to protect them against cell death [52] or kill them [61]. Because of the similarity in biological pathways between human and fission yeast, it is assumed that DIM may induce apoptosis or autophagy in fission yeast. The only study about the effects of DIM on fission yeast in 2013 shows that DIM (20µg/ml) increases chronological lifespan while a lower concentration of DIM (4µg/ml) reduces the lifespan in fission yeast [72]. This study explained the long-term effects of DIM on stationary-phase cells only. It mentioned that DIM induces anti-oxidant pathways which may be the reason to extend lifespan in fission yeast [72]. However, there is no information about the acute effects of DIM on fission yeast, therefore, I used DIM in two different concentrations 20µg/ml and 5µg/ml in log-phase cells. In this chapter, I will explain my study about investigating the new aspects of DIM on fission yeast.

I found that the effects of DIM on log-phase cells are dose-dependent. DIM induces apoptosis (20µg/ml), while the low concentration (5µg/ml) causes autophagy in log-phase cells. My results suggest that NE is one of the earliest targets of DIM and only 10 min treatment with DIM (20µg/ml) is enough to trigger apoptosis in log-phase cells. My studies on a low concentration of DIM (5µg/ml) implied that the autophagy pathway, but not the ER stress response pathway, is required for the resistance to DIM. Moreover, in this study, I showed that Lem2 is needed to resist the low concentration of DIM.

2.2. Material and method

Name	Genotype	Source
975	h^+	M. Yanagida
FY7455	h^+ *leu1-32 ura4 -D18 his7 lys1-131*	NBRP
htb1-GFP	h^+ *leu1-32 ura4-D18 his7 lys1*$^+$*::(hta1 htb1-GFP)*	
FY17186	h^{90} *ade6-216 leu1-32 lys1-131 ura4-D18*	NBRP
GFP-atg8	h^{90} *ade6-216 leu1-32 ura4- D18 lys1*$^+$*::Pnmt41-GFP-atg8*$^+$	This study
*GFP-atg8 ire1*Δ	h^{90} *ade6-216 leu1-32 ura4- D18 lys1*$^+$*::Pnmt41-GFP-atg8*$^+$ *ire1::Kanr*	This study
*ire1*Δ	h^{90} *ade6-216 leu1-32 ura4- D18 lys1-131 ire1::Kanr*	This study
*atg7*Δ	h^{90} *ade6-216 leu1-32 ura4- D18 lys1-131 atg7-d1::Natr*	This study
FY29360	h^{90} *hat1*$^+$*::GFP-Kanr ark1::Kanr-Prad21-ark1*$^+$ *atg7-d1::Natr*	NBRP
yPK002	h^+ *ade6-M210 ura4-D18 leu1-32 ire1::Kanr*	P. Walter
YT2416	h^- *lem2::Kanr*	Y. Hiraoka
80-G10	h^+ *ade6-210 leu1-32 cut11::cut11*$^+$*-GFP-HA-Kanr sid4*$^+$*-mCherry<<Natr*	Lab stock
81-D02	*h+ leu1-32 cut11::cut11*$^+$*-GFP-HA-Kanr sid4*$^+$*-mCherry<<Natr lem2::Kanr*	This study

1-1-1	*h$^+$ ade6-210 leu1 ura4 lys1 his7$^+$::lacI-GFP sod2.proximal[::Kanr-ura4$^+$-lacOp] sid4::sid4$^+$-GFP-natMX6 gar2::gar2$^+$-mCherry-hphMX6*	Ito *et al*. 2019
78-A02	*h$^+$ ade6-210 leu1 ura4 lys1 his7$^+$::lacI-GFP sod2.proximal[::Bsdr-ura4$^+$-lacOp] sid4::sid4$^+$-GFP-natMX6 gar2::gar2$^+$-mCherry-hphMX6*	Lab stock
78-D01	*h$^+$ ade6-210 leu1 ura4 lys1 his7$^+$::lacI-GFP sod2.proximal[::Bsdr-ura4$^+$-lacOp] sid4::sid4$^+$-GFP-natMX6 gar2::gar2$^+$-mCherry-hphMX6 lem2::Kanr*	Lab stock
75-D09	*h$^-$ leu1-32::Ptif51-QUEEN2m::leu1+*	Ito *et al*. 2019
DY29585	*h$^-$ his3-D1 leu1-32::Pnmt1-Ost4-CFP(leu1+) Cpy1-mCherry::natMX*	Li-Lin Du

2.2.1. Strains construction

Briefly, to express GFP-tagged Atg8, pHM43 plasmid containing a *GFP-atg8* gene with the nmt41 promoter, gifted by Dr. Yamamoto [34], was digested with New England Biolab product kit. 10 µl of X.B 2.1 buffer, 40 µl of plasmid (1000 ηg), 1 µl of EcoRI enzyme, and 50 µl RNase free water were mixed in a microtube. The sample was kept in for 4 hrs at 37^{o}C. The result of the digestion reaction was checked by electrophoresis to see the linear plasmid. After checking the quality of digestion, a linear plasmid was purified by the ethanol precipitation method and used

for transforming the cells of wild-type strain (FY17186) with "*S. pombe* Transformation Kit Wako" (See the appendix for protocols). The colonies were selected on PMG plates without lysine, which was a selective marker to screen the cells with the correct *GFP-atg8* integration.

To construct the *ire1Δ::Kanr* strain, the genomic DNA from yPK002, as a template gifted from Dr. Walter [73], was amplified by polymerase chain reaction (PCR), the primers 5'-TGGATGACTATACCCAAAGC-3' and 5'-ATCCAACGATCCCACAAGCG-3' used as primers. The resulting PCR product was introduced into the FY17186 strain by using Wako transformation kit (See the appendix for details). A YEA plate containing Kan, was used for the primary selection for colonies (See the appendix). Then deletion was confirmed by a PCR, using 5'-TAGGTATGGCCGTAGACA-3' as a forward primer. PCR program was set up with the default program as described in appendix. The annealing temperature was assigned to 52°C for 30 sec, and the extension step was at 72°C for 4 min.

The autophagy mutant, *atg7Δ*, was constructed using 5'-ATACGTAGAACTGCGGTGAG-3' and 5'-CAAATGCAACTTCAGGATCC-3' as primers. The mutated genomic DNA from *atg7-d1::Natr* strain (FY29360) was used to amplify and introduce into the wild-type strain, FY17186 with Wako transformation kit (See the appendix for protocols). A YEA plate containing Nat,

was used for the primary selection for colonies (See the appendix). Then deletion was confirmed by a PCR using 5'-CCACGGTCAAGAGTTTCAAA-3' primer as a forward primer. The annealing temperature was assigned to 52°C for 30 sec, and the extension step was at 72°C for 3 min.

2.2.2. Viability assay by spot test

For viability assay by spotting, the fission yeast cells were grown overnight at 30°C (12～15 hours) in an 8 ml of liquid YEA medium (see the appendix for media) to get the log-phase cells (0.5～1×10^7 cells/ml) designated as day0.

The culture was divided into two flasks. The same volume of Dimethyl sulfoxide (DMSO) or 20 μg/ml DIM, purchased from Combi-Blocks (San Diego, USA) dissolved in DMSO, were added to each flask. On day1, which was 24 hours after incubation with the drugs, the cell number was adjusted to 1×10^7 cells/ml and used for viability assay with five-fold serial dilutions. The spotted plates were incubated at 30°C for 3 to 5 days to check cell viability. Every 24 hours, the viability assays were repeated till day9. For the stationary-phase cells, before adding the drugs, untreated day1 cells, containing about 1×10^8 cells/ml, were spotted in five serial dilutions (the cell number was adjusted to 1×10^7 cells/ml for spotting assay). Then DIM and DMSO were added into 3ml of day1 cells in individual utensils. 24 and 48hrs after adding the drugs, spotting assays were repeated for treated cells and incubated at 30°C for 3 to 5 days to take images.

2.2.3. Acute viability assay by spot test

The log-phase (day0) and stationary-phase cells (day1) were prepared by YEA medium. After adjustment of cell concentrations (1×10^7 cells/ml) in one sample tube, immediately, DMSO or DIM (20 and 40 μg/ml) were added to the cultures and incubated for 10 min at 30°C. After precipitating, washing the drugs with sterile water, and suspending with YEA and counting the cell concentration, 100 μl of treated cultures with the same concentration (1×10^7 cells/ml) were used for viability assay. Spot assays were done in five-time serial dilutions on YEA plates and saved at 30°C for 3 to 5 days to take the images.

2.2.4. Quantitation of the percentage of viability

The liquid YEA medium containing 3% of glucose was used for overnight culture in each strain and then they were treated based on the desired experiment in three independent replications. The same cell number (500 cells) for each treatment were dispersed on YEA plates, after counting the cells number with a hemocytometer. Three days later, the grown colonies were counted and the viability percentages were calculated. The percentage of viability at day 0 (= reaching the log-phase) was set to 100% of viability, and subsequent grown colonies number was normalized to day 0 when the drugs were added to the log-phase cells. In the case of stationary-phase cells, the percentage of viability was normalized at day 1 (=

reaching the stationary-phase), and the viability percentage for day 1 was set to 100% and subsequent grown colonies number was normalized to day 1.

Percent of viability for *atg7Δ*, *ire1Δ*, and *lem2Δ* strains compared to wild type have been measured three days after adding DMSO, DIM (5 µg/ml), or 2-ME (10 mM) to the log-phase liquid cultures.

2.2.5. Apoptosis detection by acridine orange/ethidium bromide (AO/EB) and 4',6-diamidino -2-phenylindole

Dual staining by AO/EB was conducted to detect dead cells and terpinolene (300 mg/l), Tokyo Chemical Industry Co (TCI), was used as control to show apoptosis phenotype [14]. AO was purchased from FUJIFILM Wako Company in Japan. Briefly, after precipitation with 2 min centrifuge (3,000 rpm) and washing the 20hrs-trated cells with PBS (pH: 7.4), cells were resuspended in 100 µl PBS with 5 µl of AO/EB mixture (AO 60 µg/ml: EB 100 µg/ml). Five min after incubation in the darkroom at room temperature, cells were washed twice with 300-500 µl of PBS and precipitated with 1 min centrifuge (3,000 rpm) and imaged by a Zeiss GFP filter set 38 HE of fluorescence microscope for AO, and a Zeiss mRFP filter set 63 HE for EB. 1 µl of AO stock (600 µg/ml) and 1 µl of EB stock (1 mg/ml) and 8 µl of PBS were used as AO/EB mixture for every 1 ml culture. Terpinolene stock was prepared by dissolving in DMSO. Exposure times were set at 400ms for GFP, 200ms for RFP, and 400ms for the DIC channel. Totally, EB is up taken by dead cells only because

of membrane integrity loss in dead cells, but AO permeates into both dead and live cells and stains them green. Finally, dead cells are detectable in orange color in the merged images. Images were analyzed by ImageJ software.

To visualize nuclear fragmentation and condensation, 1 ml of the cultures were precipitated with 2 min centrifuging at 3,000 rpm, after discarding the medium, 1 ml milli-Q water was used to wash the pellets. After 2 min centrifuging, plates were suspended with 300 µl of 70% ethanol, and kept at 4°C for 20 min. After precipitation of the cells with centrifuging (2 min, 3,000 rpm), the precipitated cells were mixed with DAPI (0.1 mg/ml) in a 1:1 portion ratio to stain chromosomes. Stained cells were transferred on a glass slide and nuclei were observed under a fluorescence microscope. For microscopic analysis, a Zeiss microscope and the AxioVision 4.8 software were used to capture images, which were then analyzed using the ImageJ software.

2.2.6. Microscopy

Basically, 1ml of the desired treatment or control cultures were used and precipitated by centrifuge at room temperature for 1 min (3,000rpm), then transferred on a glass slide, and checked by a related filter set with a Zeiss microscope with AxioVision 4.8 software. In the timelaps monitoring, 2 min interval was used.

2.2.7. ATP level measurement

YEA log-phase culture was prepared for strain 75-D09 [74] with expressing of Queen. Cells were treated with DMSO, DIM (20µg/ml) and sodium azide (NaN3, 0.2mM) separately and incubated for 10 and 20 min at 30°C. 1ml of each culture was used to check and take the images with fluorescence microscopy. Queen is an ATP biosensor with two excitation peaks (410 ηm for joined ATP with Queen and 480 ηm for Free Queen), the mean ratio for these two excitation peaks gave an estimation for ATP level in cells [75]. After the image processing, the color of the cell with the normal ATP level was green and the color of cell with the low or without ATP level was blue (Fig. 2.2).

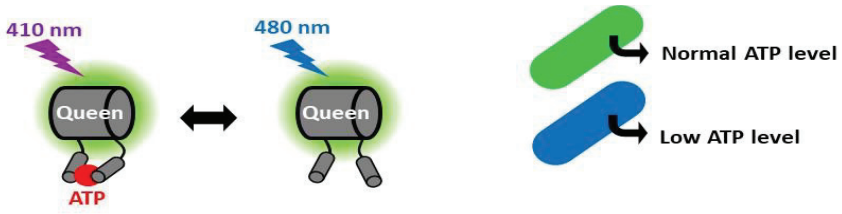

Fig 2.2. Design of Queen. The highest signal intensity (excitation peak) of ATP-bound Queen is at 410 ηm, while for of free Queen is at 480 ηm [75]. The mean ratio for these two excitation peaks gave an estimation of ATP level in the cell. After image processing, cells with normal ATP level are in green color, in contrast to the cells with low ATP level are in blue color.

To take the image, two different filter set was used. The first filter set was custom-made filter set CHROMA (ET 395/25×/BS T495lpxr/EMET525/50m). A

Zeiss GFP filter set 38 HE was also used [74], and the light exposure times for the DIC channel were decreased to 2ms in comparison to 80ms for CHROMA or 300ms for the GFP channel. Data were analyzed in ImageJ software. Before analysis, the "Adjustable Watershed" plugin was installed to the software, and "Rainbow Smooth.lut" was attached by copying and pasting the file in "luts" folder. With "drag and drop", zvi images were opened in software. The stack viewing and the color option were set as "Hyperstack" and without autoscale respectively. Images were split into different channels through the Image>Color> Split channels. After splitting the channels, three separated channel were created.

C1- (file name) = 400 nm excited image, for DAPI channel

C2- (filename) = 480 nm excitation image, for GFP channel

C3- (file name) = for DIC image

For every channel, these three steps were done through the

①Process>Subtract Background>Rolling ball radius=50.0 pixel.

②Image>Type>32bit

③Image>Adjust>Threshold > Dark Background>Auto>Apply>Set to NaN

Then a new window was created through the Process>Image calculator. For Image1: C1 and Image2: C2 were selected and dividing operation was run. Through the Image>lookup Table, "Rainbow Smooth" was selected. Over the

Image>Adjust>Brightness and Contrast>, the minimum was set to =0, and the maximum was set as =4. Every cell was selected by using the freehand selection option from the toolbar. To analyze the data, the Analyze>Measure was used and the mean values were considered as a real data. The black area was NaN and the area was considered to be 0, therefore, it was not necessary to surround the cell exactly according to the outline.

2.2.6. Nitrogen starvation and the condition in which DIM induces autophagy

The overnight culture in PMG medium (see the appendix for media), supplemented by nucleotides and amino acids, was used to get log-phase cells of the GFP-Atg8 strain. 4 ml of the culture were precipitated and washed (2min, 3,000rpm). Medium was replaced by EMM with 1% glucose without any source of the nitrogen and incubated at 30°C. In parallel, 5 μg/ml DIM and DMSO were added to 4 ml of the overnight cultures in PMG (~0.5×10^7 cells/ml) and incubated at 30°C in PMG. GFP-Atg8 foci were monitored by a fluorescence microscope after four hours of nitrogen starvation and two hours of incubation with DIM, respectively.

2.2.7. Viability assay by spot test in DIM autophagy inducing condition

In viability assay, 3% YEA liquid medium was used, and fresh YEA plates were employed, containing the 5 μg/ml DIM or DMSO for the control condition. DIM was added to the solid YEA medium when it was warm (not hot) just before

pouring into the plates, and DIM plates were saved at room temperature or 4°C far from light, (they were usable at least for 2 days). For spotting assay, log-phase cells were used and after spotting, in five-time serial dilutions, plates were incubated at 30°C for 3-5 days to take images. To compare the ER stress induction, the fresh plates with 10 mM 2-mercaptoethanol (2-ME) were used.

2.2.8. Statistical analysis

The post hoc T-test with Bonferrori correction was used to compare between the treatments or genotypes. All of the statistical analyses were done in excel software.

2.3. Results and discussion

2.3.1. DIM reduces cell viability in log-phase cells, but not in stationary-phase cells

A study has shown that a high concentration of DIM (20 μg/ml) increases chronological lifespan in fission yeasts while a low concentration of DIM (4 μg/ml) seems to reduce lifespan [72]. These facts imply that DIM may have both positive and negative effects on cell viability in fission yeast. Chronological lifespan is investigated using stationary-phase cells. However, the acute effects of DIM on fission yeast log-phase cells are not reported. To understand the early effects of DIM on fission yeast cells, first I carried out a viability spotting assay by focusing on the log-phase stage. In this case, DIM (20μg/ml) was added to the day 0 culture which contained log-phase cells (0.5 to 1×10^7 cells/ml) and after one day, spotting assay was done with five-fold serial dilutions (Fig. 2.3A). Surprisingly, when cells were cultured for only 24 hours in the presence of a high concentration of DIM (20μg/ml), cell viability was reduced dramatically (Fig. 2.3A, day 1) and severe growth defect was observed during the first 24 hours (Fig. 2.4). To quantify the amount of viability reduction and to show DIM does not arrest the growth, the percentage of viability was analyzed based on counting the colony formation (Fig. 2.3B). As shown, results indicated significant viability reduction during first 24 hours after adding the DIM (20μg/ml) (Fig. 2.3B, day 1). To know for how long DIM has the negative effects on

viability, the spotting assays were performed till day 9 and quantified by counting the colonies (Figs. 2.3A and B). As shown previously [72], my results also showed that the cell viability was better in the presence of a high concentration of DIM (20µg/ml) in comparison to DMSO condition after day 5 (Figs. 2.3A and B). Surprisingly in DIM condition, no viability reduction was observed on day2 in comparison with day1 (Figs. 2.3A and B).

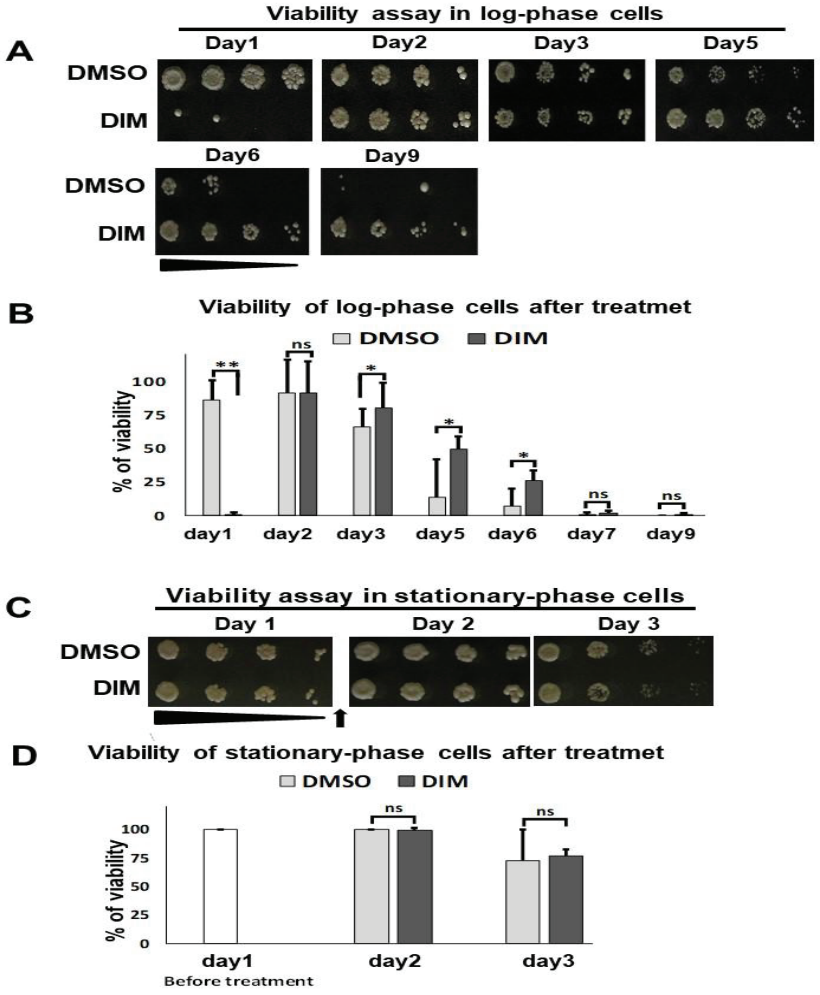

Fig 2.3. DIM inhibits the cell viability of log-phase cells. (A and B) DIM (20 µg/ml) was added to the log-phase cells (~0.5-1 x 10^7 cells/ml) and spot assay with five-fold serial dilutions was

conducted for viability test (A). For control experiment, Dimethyl sulfoxide (DMSO) was used. The cell viability with the same cell concentration was done on YEA plates during nine days**.** 24 hours incubation after adding the drug was named "Day 1". Percentages of viability for each day are shown (B). (C and D) DIM (20 µg/ml) was added to the stationary-phase cells and the viability was studied (C). Log-phase cells were cultured for 24 hours. Then, DIM (20 µg/ml) was added to the stationary-phase cells (~1 x 10^8 cells/ml). The cell viability was checked with same cell concentrations till day 3**.** Arrow shows the time of adding DIM. Percentages of viability of treated stationary-phase cells are shown in D. See materials and methods for details.

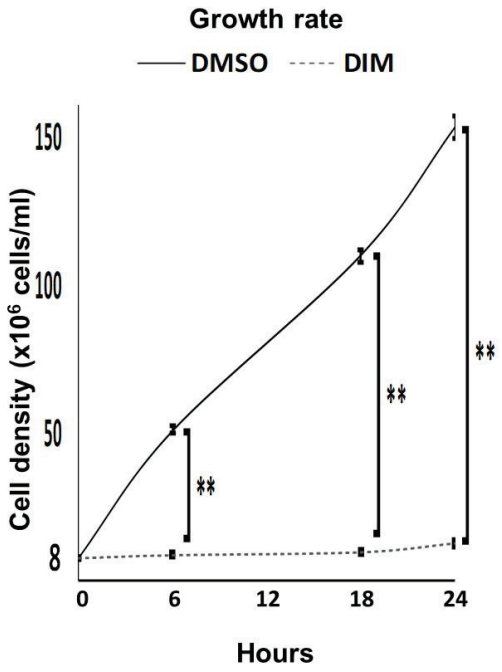

Fig 2.4. DIM inhibits cell growth in log-phase cells during the first 24 hours. DIM (20 µg/ml) was added to the log-phase cells and the cell growth was measured during the first day.

It indicated that DIM did not inhibit cell growth after additional incubation on day 2 (Figs. 2.3A and B) and suggested that either DIM does not decrease the viability when cells are in the stationary-phase or DIM is decomposed. To test the possibility that a high concentration of DIM does not reduce the cell viability when the cells are in the stationary-phase, DIM (20μg/ml) was added to the stationary-phase cells which were day1 cells (~1×10^8 cells/ml). I found that DIM did not reduce the viability of the cells in stationary-phase on day 2 in comparison with the viability of the cells day1, before treating (Figs. 2.3C and D).

2.3.2. Acute effect of DIM on log-phase and stationary-phase cells

One of the possibilities that stationary-phase cells are resistance to DIM is higher cell number in stationary-phase culture, which may reduce the effective concentration of the DIM relative to each cell. To test this possibility, an acute viability assay was performed (Fig. 2.5). The same cell number were adjusted between stationary- and log-phase cells and I incubated them with DIM (20μg/ml) just for 10 min to avoid cell phase-shifting of stationary-phase culture. Then DIM was removed with wash out the cells and spotting assays were done.

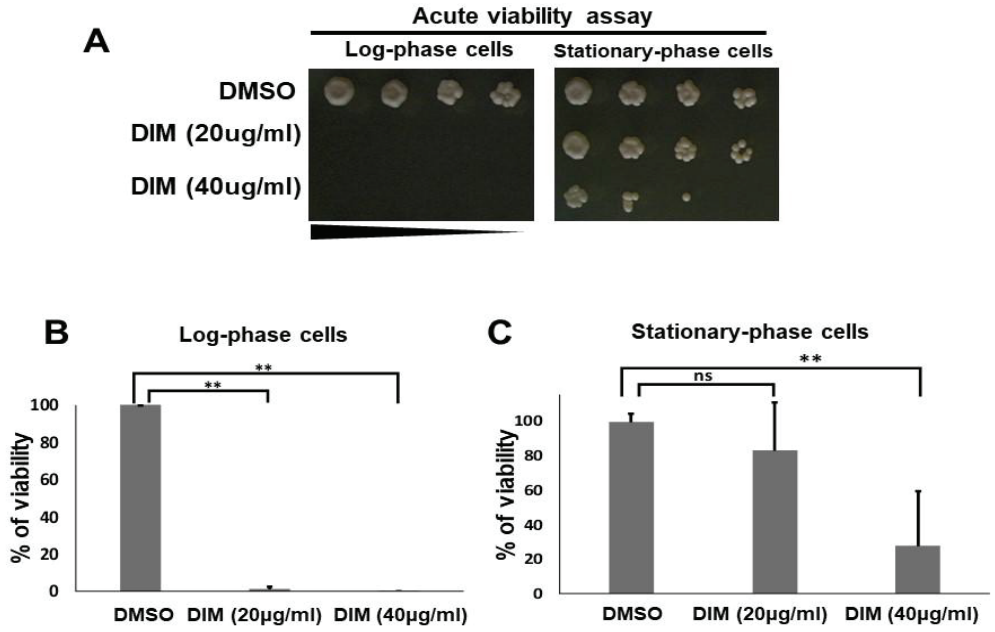

Fig 2.5. Ten minutes incubation with DIM is enough to kill log-phase cells. (A) The same concentration of log-phase cells and stationary-phase cells (1 x 10^7 cells/ml) were incubated in the presence of DIM (20µg/ml) or DMSO for 10 min to do the acute viability assay. Images were taken after 3 to 5 days incubation at 30°C. (B and C) The percentages of viability are shown as A for the treatments. See materials and methods for details.

The result showed that the ratio of drug molecules per cell is not the reason for the difference in viability of log-phase and stationary-phase cells in response to DIM (Figs. 2.5A) and stationary-phase cells are still more resistant to DIM than log-phase cells when 20µg/ml or 40µg/ml DIM was used. 10 min of incubation with DIM was also enough to trigger cell death in log-phase cells (Figs. 2.5B), it means the process of cell death, continues even after DIM removal.

As it implied, the stationary-phase cells were more resistant to DIM than the log-phase cells with the same cell concentration (Figs. 2.5A and C, DIM 20µg/ml). However, even the higher concentration (40 µg/ml) of DIM killed the stationary-phase cells (Figs. 2.5A and C), demonstrating that DIM affects viability of stationary-phase cells when the DIM concentration is very high.

2.3.3. DIM is suggested to induce apoptosis in log-phase cells

The recent results from human studies showed that DIM induces apoptosis in various cancer cells by different mechanisms [55, 76]. It was assumed that DIM possibly kills the fission yeast by apoptosis induction. To ask about this possibility, I checked the vital status of 20hrs-treated cells in log-phase and stationary-phase cultures through the dual staining method with AO and EB (see material and method [14]). As it mentioned in material and method section, only the dead cells are stained by ethidium bromide. Dual staining demonstrated about 100 percent of cell death in both log-phase and stationary-phase cells by terpinolene (300 mg/ml), which is an apoptotic inducer and used as a control compound [14] (Figs. 2.6A and B). I found about 80 percent of log-phase cells died after 20hrs of incubation with DIM (20µg/ml) (Figs. 2.6A and B), in contrast, stationary-phase cells were not killed by DIM (Figs. 2.6A and B). Nuclear fragmentation is a hallmark of apoptotic cell death in fission yeasts [19]. Therefore, to investigate apoptosis induction, the shape of the nuclei was analyzed by DAPI staining in the log-phase and stationary-phase cultures

that were incubated for 6hrs with DIM (20µg/ml), DMSO, and terpinolene (300mg/ml). Terpinolene induced nuclear fragmentation and apoptosis [14] in both log-phase and stationary phase cells (Figs. 2.6C and D). I detected nuclear fragmentation in log-phase cells (Figs. 2.6C and D). The metacaspase activity as a sign of apoptosis was not compared in my experiments. Considering that DIM induces caspase activity in human cancer cells [46-47], my indirect results suggested that DIM may induce apoptosis in log-phase cells in fission yeast (Figs. 2.6C and D). In contrast, there was no difference in nuclei morphology between DMSO and DIM treated stationary-phase cells. Therefore, my results implied that DIM may induce apoptosis in the log-phase cells but not in the stationary-phase cells.

Moreover, based on the acute assay result (Fig. 2.5), treatment with DIM (20µg/ml) for 10 min with DIM is enough to reduce cell viability in log-phase. However, it was unknown if this 10 min treatment also triggers apoptosis in log-phase cells. To ask it, first dual staining was done in log-phase cells which were treated for 10 min with DIM (20µg/ml) (Fig. 2.7). I found that 10 min-treated cells were not stained by ethidium bromide, suggesting that the cell membrane remains intact and DIM does not kill the cells within 10 min instantly (Fig. 2.7A). In addition, 10 min-treated cells, were precipitated and washed, and cells were transferred to the solid YEA medium for 6hrs, after it, nuclear fragmentation was measured in them. I found that even when 10 min treatment with DIM (20µg/ml)

could not kill the cell immediately (Fig. 2.7A), however, it was enough to trigger nuclear fragmentation in cells after 6 hours (Fig. 2.7B).

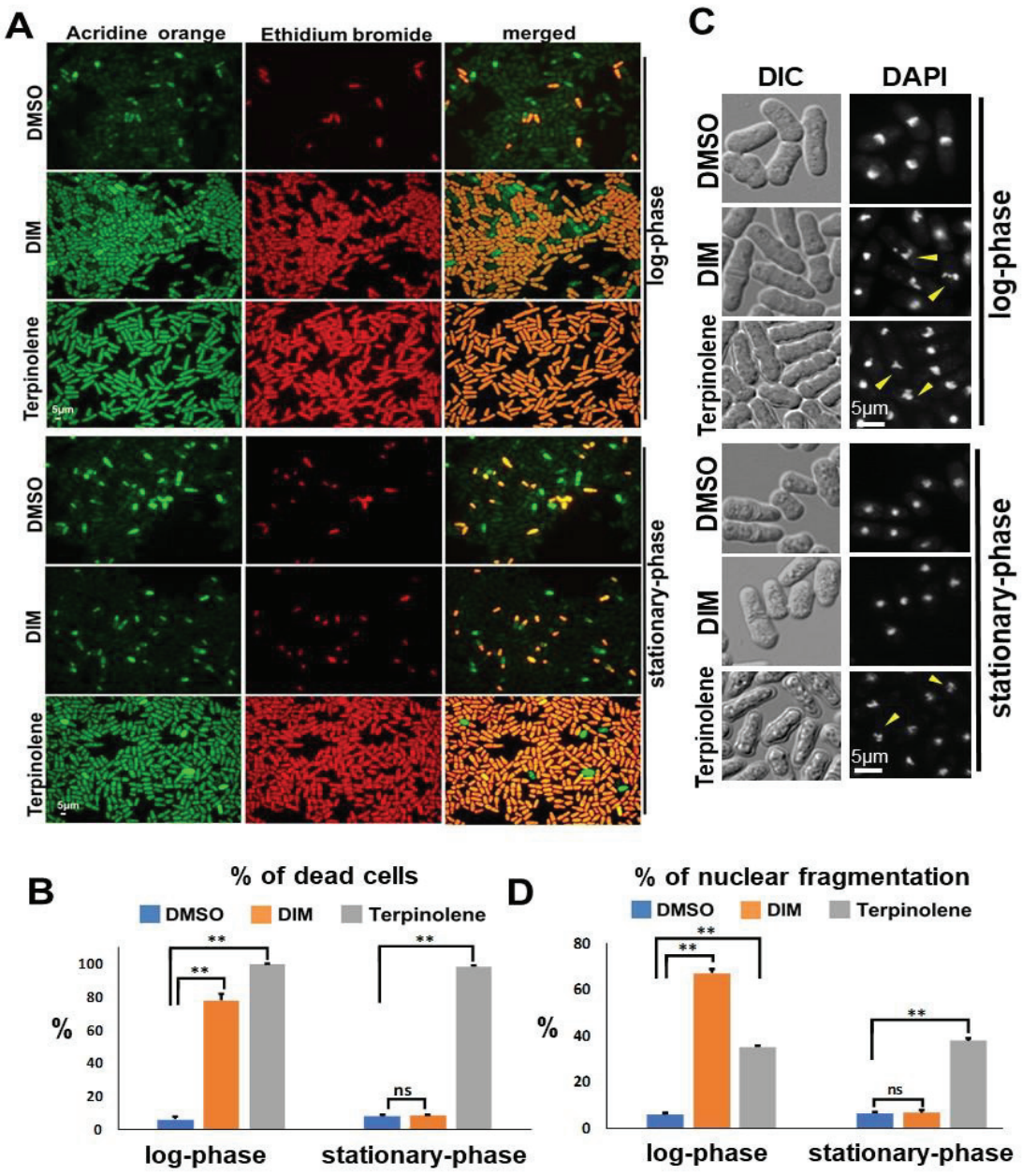

Fig 2.6. DIM induces apoptosis in fission yeast log-phase cells. (A and B) 20 hours after adding DIM (20 µg/ml), the cells were stained with AO and EB. Terpinolene (300 mg/l) was used as a control positive treatment. Details about microscopy and imaging were described in material and method section (A). The percentages of dead cells were calculated from the merged images using ImageJ software is shown in B. At least 300 cells were counted with three independent experiments for comparison. (C and D) DAPI staining was used to detect the nuclear fragmentation after six hours of incubation with DIM (20µg/ml) or terpinolene (300 mg/l) (C). The percentages of nuclear fragmentation are shown in D for at least 200 cells were with three independent experiments.

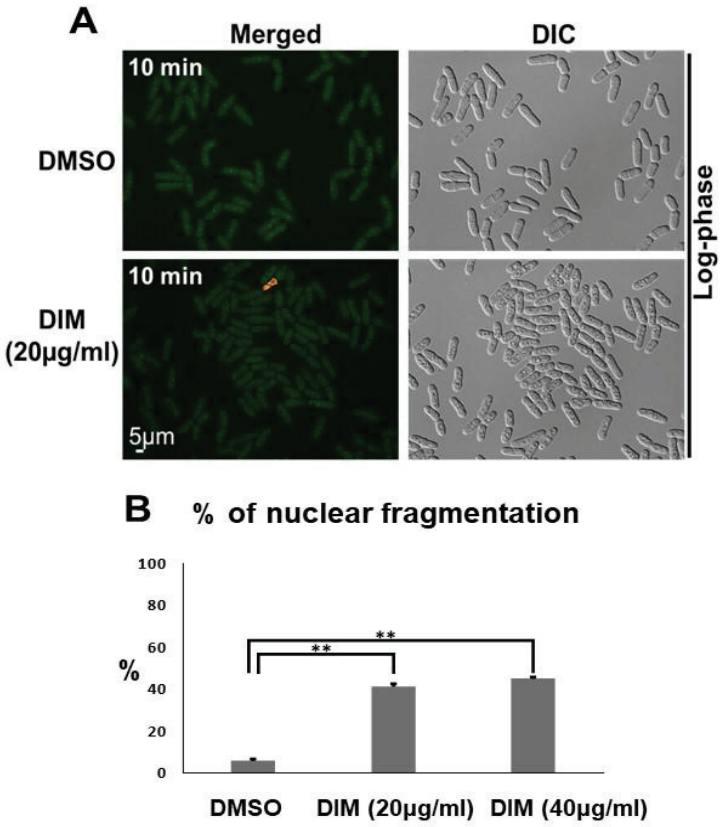

Fig 2.7. DIM triggers cell death but cell membrane integrity is not destroyed at an early time point. (A) The log-phase culture was prepared for wild type and treated with DIM (20 µg/ml) and

incubated for 10 min. Dead cell abundance was detected with dual staining method as shown in orange color. The percentages of nuclear fragmentation are shown in B. The log-phase cells were treated with DIM (20 μg/ml and 40 μg/ml) for 10 min. After treatment, cells were washed, precipitated, and transferred to the sample tubes containing sold YEA medium. Six hours later, nuclear fragmentation was monitored by DAPI staining. For compassion, at least 200 cells were counted with three independent experiments.

2.3.4. DIM induces nuclear condensation and NE disruption in log-phase cells within ten minutes.

To understand how DIM caused the reduction in viability of log-phase cell (Figs. 2.3A and B, day 1), I analyzed nuclear morphology using cells expressing histone H2B fused to GFP (Htb1-GFP) in the presence of DIM or DMSO (Fig. 2.8). More than 98 percent nuclear condensation was observed in the log-phase cells which were incubated for 10 min by DIM (20 μg/ml) (Figs. 2.8A and D) in contrast to stationary-phase cells (Figs. 2.8C and D). I analyzed NE morphology using a strain expressing Cut11-GFP in DIM condition. The result from analyzing the cut11-GFP strain, suggested that DIM may disrupt NE in log-phase cells within 10 min (Figs. 2.8B and E) but not in case of stationary-phase cells (Figs. 2.8C-E).

The difference in the nature of NE, gene transcription or protein compositions of cells might be the reason for the sensitivity of log-phase cells in comparison to stationary-phase cells. Ish1, a NE protein, has a higher level of expression in stationary-phase than in log-phase [77]. Ish1 may be a candidate for the resistance to

DIM in stationary-phase cells. However, it is possible that DIM targets the unknown NE-independent protein(s) in log-phase cells, which may be absent in stationary-phase cells.

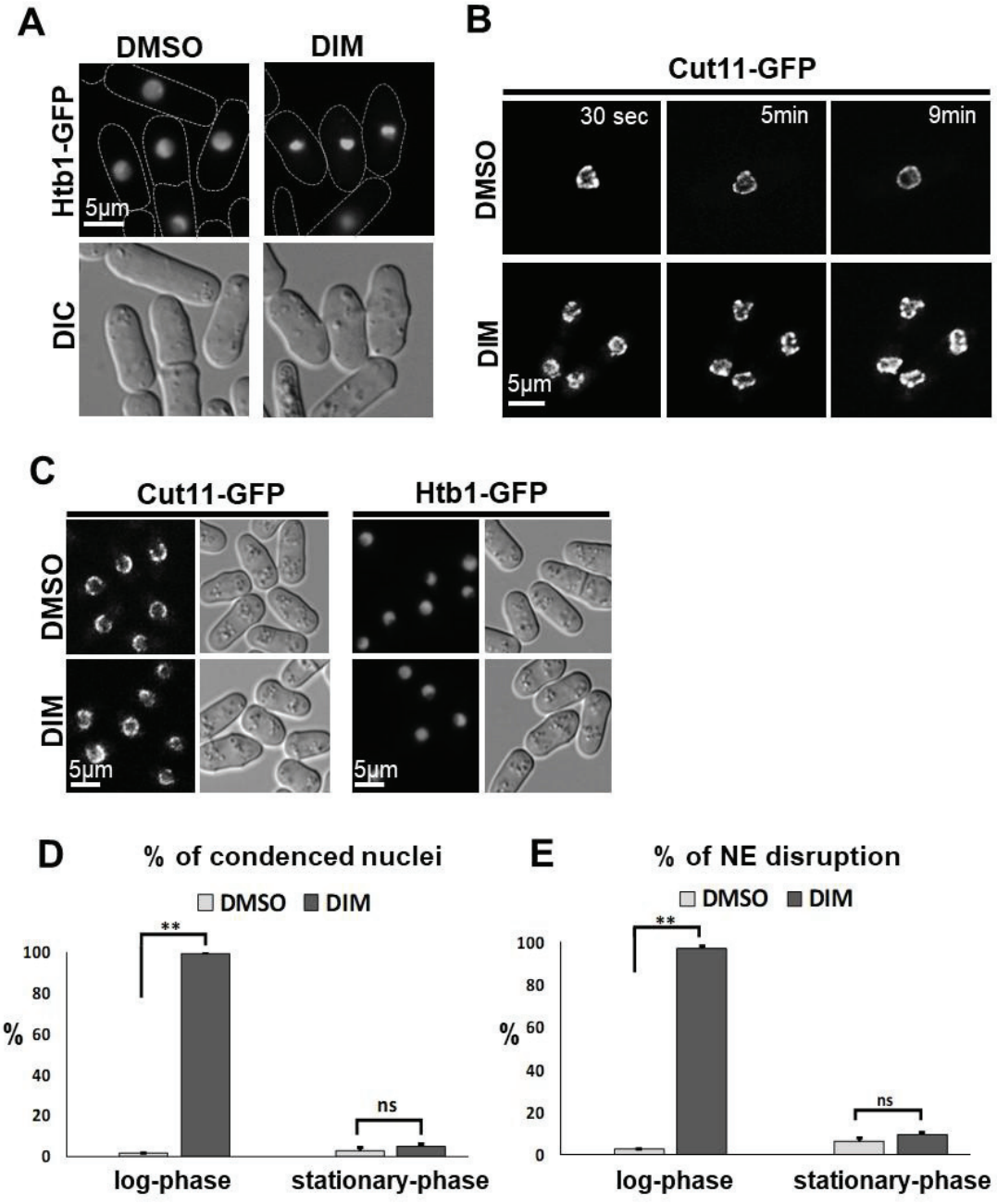

Fig 2.8. DIM induces nuclear condensation and NE disruption in log-phase cells. (A) DIM (20 μg/ml) was added to log-phase cells (0.5～1 x 10^7 cells/ml) expressing Htb1-GFP as a histone marker. (B) The time-lapse images taken during the 10 min incubation with DIM (20 μg/ml) and DMSO, using Cut11-GFP signal as a marker for nuclear envelope (NE). (C) DIM (20 μg/ml) was added to the stationary-phase cells (10～15 x 10^7 cells/ml) that are cultured as in Fig. 2.3C. After 10 min, the shape of the nuclei and NE were observed as in A and B. (D and E) At least 200 cells were counted with three independent experiments for D and E separately, to calculate the percentages of condensed nuclei and possible disrupted NE in log- and stationary-phase cells.

Moreover, it is possible that DIM inhibits some of the membrane proteins that are required for NE integrity, or suppresses the pathway(s) involve in control of the protein transportation between nucleus and cytoplasm at DIM (20 μg/ml) condition. Thus, DIM may cause the mis-localization of the nuclear or cytoplasmic protein by the possible disrupted NE. Subsequently, this mis-localization may change nuclear homeostasis and induce nuclear condensation. Nuclear condensation and NE disruption are known as signs of apoptosis induction in fission yeast [15, 17, 19]. However, in my experiments, both these signs happened much earlier than previous observations [15, 17, 19]. It is known that the disruption of nuclear transport and disassembly of the nuclear pore complex (NPC) occurs before caspase-9 activation in humans [78]. In conclusion, it could be possible that during the first 10 min treatment of fission yeast cells by DIM, both nuclear condensation and NE disruption happen before apoptosis induction. NE disruption by DIM and possible

subsequent defect in protein transport between the nucleus and the cytoplasm might be a reason for apoptosis induction. Further studies are necessary to understand the mechanism of apoptosis induction by DIM in fission yeast.

2.3.5. Mitochondrial ATPase may not be the first target of DIM in fission yeast.

Previous studies have shown that one of the direct targets of DIM in human cells is mitochondrial F1F0-ATPase [54] which reduces ATP level and induces cell arrest in MCF-7 breast cancer cells [55]. To ask if DIM inhibits mitochondrial ATPase in fission yeast or not, and whether ATPase is the early target of DIM in vivo condition, I measured the ATP level after adding the DIM (Fig. 2.9). I used a strain, which has a Queen as a reliable ATP biosensor [74]. Queen has two excitation peaks (410 nm for bounden ATP by Queen and 480 nm for Free Queen) [75]. The mean ratio of Queen signal per cell shows ATP level. Sodium azide (NaN_3) is used as a known mitochondrial F1F0-ATPase inhibitor [79]. NaN_3 inhibits oxidative phosphorylation via inhibition of cytochrome oxidase and reduces ATP level rapidly [79]. I assumed that ATP level must be reduced by DIM rapidly similar to NaN3. To Investigate it, the log-phase cells of Queen expressing strain were treated with DMSO, DIM (20µg/ml), and NaN3 (0.2mM) separately and incubated for 10 and 20 min. Then ATP level were measured after image processing in ImageJ software (Fig. 2.9B). My results indicated that the NaN_3 reduces the ATP level

rapidly after 10 min, however, DIM (20µg/ml) causes ATP reduction after 20 min (Fig. 2.9). It implied that mitochondrial ATPase in fission yeast is not the early target of DIM, because NE disruption and nuclear condensation were observed within 10 min after treatment with DIM (Fig. 2.8), which has happened earlier than ATP reduction (Fig. 2.9).

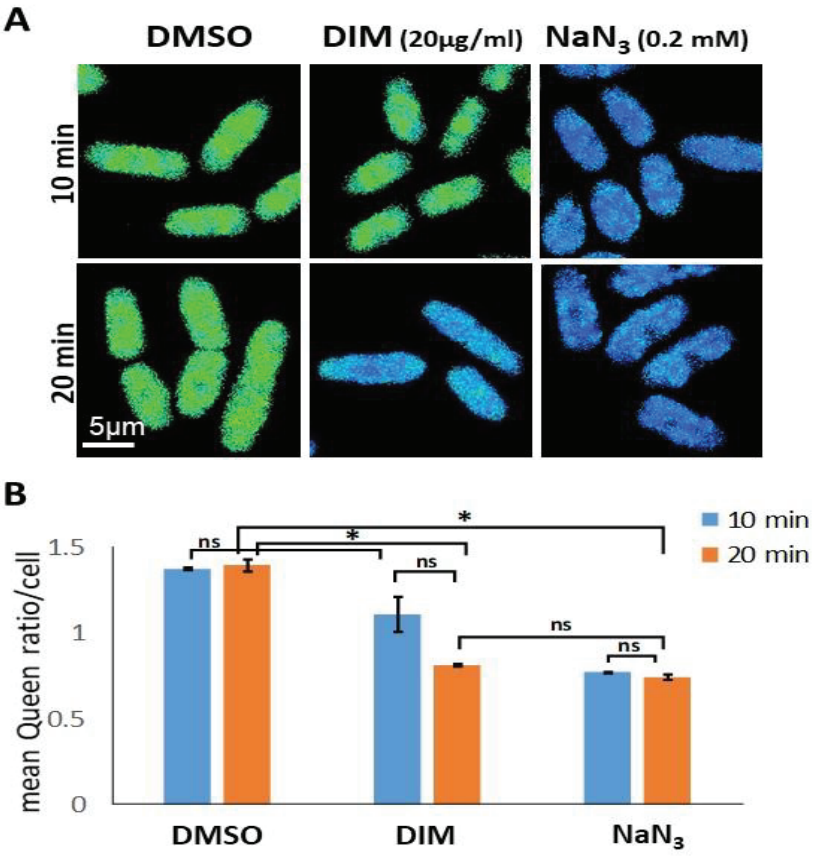

Fig 2.9. Mitochondrial ATPase is not the first target of DIM in fission yeast. (A) The log-phase culture of Queen expressing strain [74] was prepared and treated with DMSO, DIM (20µg/ml), and NaN_3 (0.2mM) separately and incubated for 10 and 20 min. The taken images were processed with ImageJ software. The green color indicates normal ATP level, and the blue color means low ATP

level in cells. (B) The mean Queen ratio per cell was compared. ATP level was measured in at least 50 cells for each treatment. See material and method for details.

2.3.6. Autophagy is induced by DIM, and the autophagy pathway but not the ER stress response pathway is required for the resistance to DIM

DIM induces autophagy in human cancer cells [61]. To understand if DIM induces autophagy in fission yeast, first, I constructed the strain expressing ectopic GFP-Atg8 with the nmt41 promoter, by integrating liner plasmid into the wild-type strain (see the material and method for details). Autophagy contributes to cell viability under nitrogen starvation in fission yeast [11]. Therefore, I checked autophagy induction through the nitrogen starvation (Fig. 2.10A). It is known that GFP-Atg8 foci are produced by nitrogen starvation in fission yeasts [26] (Fig. 2.10A), which is a hallmark of autophagy induction. However, when 20μg/ml of DIM was used, GFP-Atg8 signal was dispersed in the DIM-treated cells and it was not detectable (data not shown here), suggesting that high concentration of DIM (20μg/ml) cannot induces autophagy in log-phase cells. In contrast, I observed GFP-Atg8 foci in treated log-phase cells after two hours incubation with DIM (5μg/ml) (Fig. 2.10B). This result suggested that DIM induces autophagy in fission yeast at a low concentration (5 μg/ml).

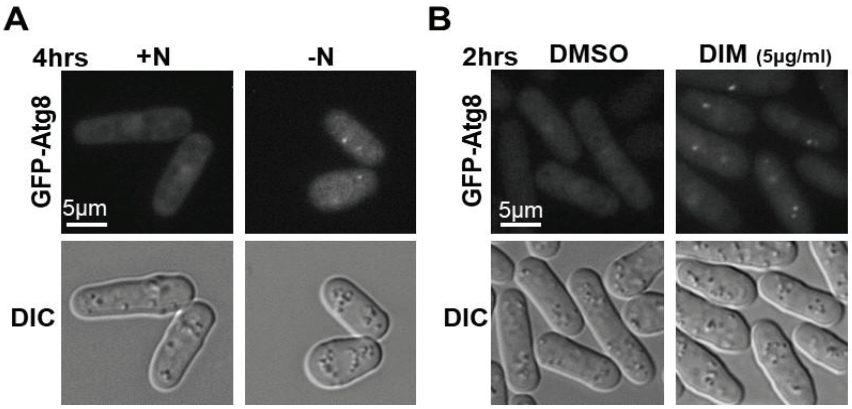

Fig 2.10. A low concentration of DIM induces autophagy in fission yeasts. (A and B) Cells expressing GFP-Atg8 were incubated for four hours in nitrogen starvation condition as a positive control condition (A) or treated a low concentration of DIM (5 μg/ml) and incubated for two hours (B). GFP-Atg8 foci were used as markers for autophagy induction. See materials and methods for details.

To ask whether autophagy induction by DIM leads to the complete process of autophagy, DY29585 strain was used [33]. DY29585 contained two protein markers, Ost4-CFP, an ER protein, and Cpy1-mCherry for vacuoles (Fig. 2.11). Co-localization of Ost4-CFP and Cpy1-mCherry means the entry of ER membrane into the vacuole and shows the degradation step of autophagy [33]. Dithiothreitol (DTT) was used as a control treatment, which causes autophagy in fission yeast [33]. As shown here (Fig. 2.11), treatment with DMSO didn't show co-localization for both markers, which means no autophagy. In contrast, after 20hrs incubation with DTT (10mM), autophagy was confirmed with co-localization of Ost4-CFP and Cpy1-mCherry. A co-localization for both markers was also found in DIM (5μg/ml)

concentration after 20hrs incubation, which means autophagy is continued by the time to complete its process.

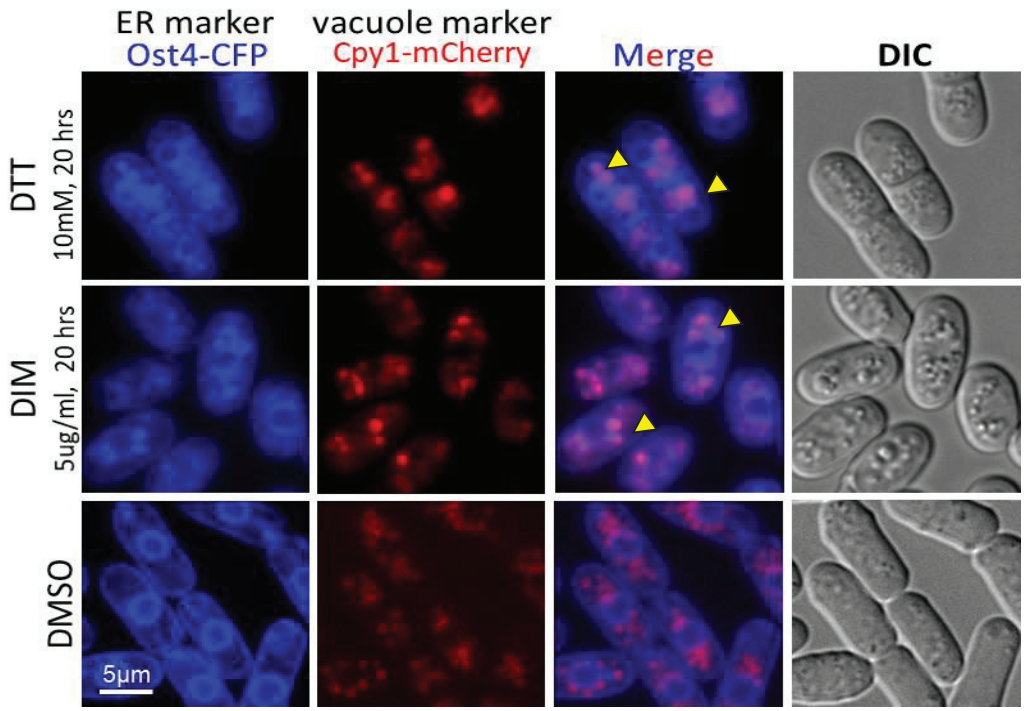

Fig 2.11. Confirmation of autophagy by DIM (5µg/ml) in log-phase cells of fission yeast. The log-phase cells were prepared with EMM medium supplemented with required nucleotide and amino acids (see media appendix). Cultures were treated with DMSO, DIM (5µg/ml) and DTT (10mM) and incubated for 20hrs at 30°C. To prevent changing the cell phase from log-phase to stationary-phase during the 20hrs, primary cell concentration was adjusted around to 0.2 x 10^7 cells/ml. Images were taken by a Zeiss CFP filter set 47 HE of fluorescence microscope for Ost4-CFP, and a Zeiss mRFP filter set 63 HE for Cpy1-mCherry and analyzed in ImageJ. See material and method for details about taking the images. Arrows show the co-localization of both markers indicating the final process of autophagy.

For the assessment of autophagy, a western blot analysis was also done for strain expressing GFP-Atg8. After 8 hrs, nitrogen starvation accumulated cleaved GFP, which indicated the autophagy process. However, only a weak band that may be cleaved GFP was detected after 15 hrs in DIM-treated cells. However, the band intensity was not strong enough for the publication grade. Therefore, the western-blot result is not shown here. Due to the other results, which indicated autophagy induction by DIM (Figs. 2.10 and 2.11), it is possible that DIM produced cleaved GFP, which may be degraded.

To investigate the contribution of autophagy in cell survival in the presence of DIM (5µg/ml), I used a constructed *atg7*Δ strain (See material and method). As shown previously, *atg7*Δ cells that have defect in the autophagic pathway, lose viability under nitrogen starvation [80] (Fig. 2.12).

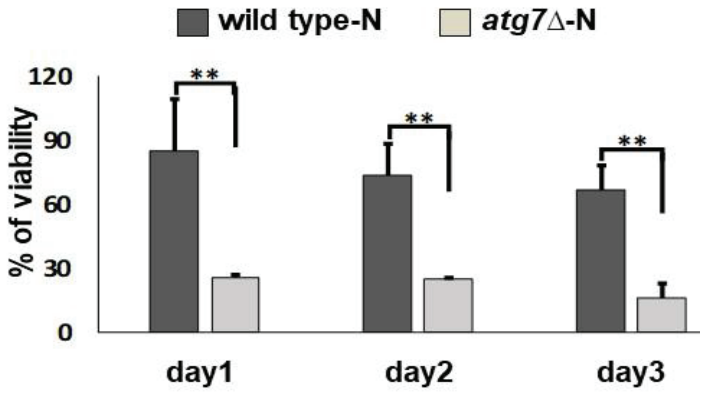

Fig 2.12. *atg7*Δ strain lose viability under nitrogen starvation. Percentages of viability under nitrogen starvation for three days are shown. The log-phase cells of auxotrophic wild type strain (h^{90} *ade6-216 leu1-32, ura4-D18, lys1-131*) and its *atg7*Δ mutant were cultured in YEA medium. Then

cells were cultured in EMM without any nitrogen source and adenine, leucine, uracil and lysine. Day1 means that cells were cultured for one day under nitrogen starvation.

Using the spotting assay (Fig. 2.13A) and calculating the viability percentage (Fig. 2.13C) showed that *atg7*Δ cells are more sensitive to low concentration of DIM (5 μg/ml) than wild-type cells. It means the autophagy pathway contributes to the resistance to a low concentration of DIM.

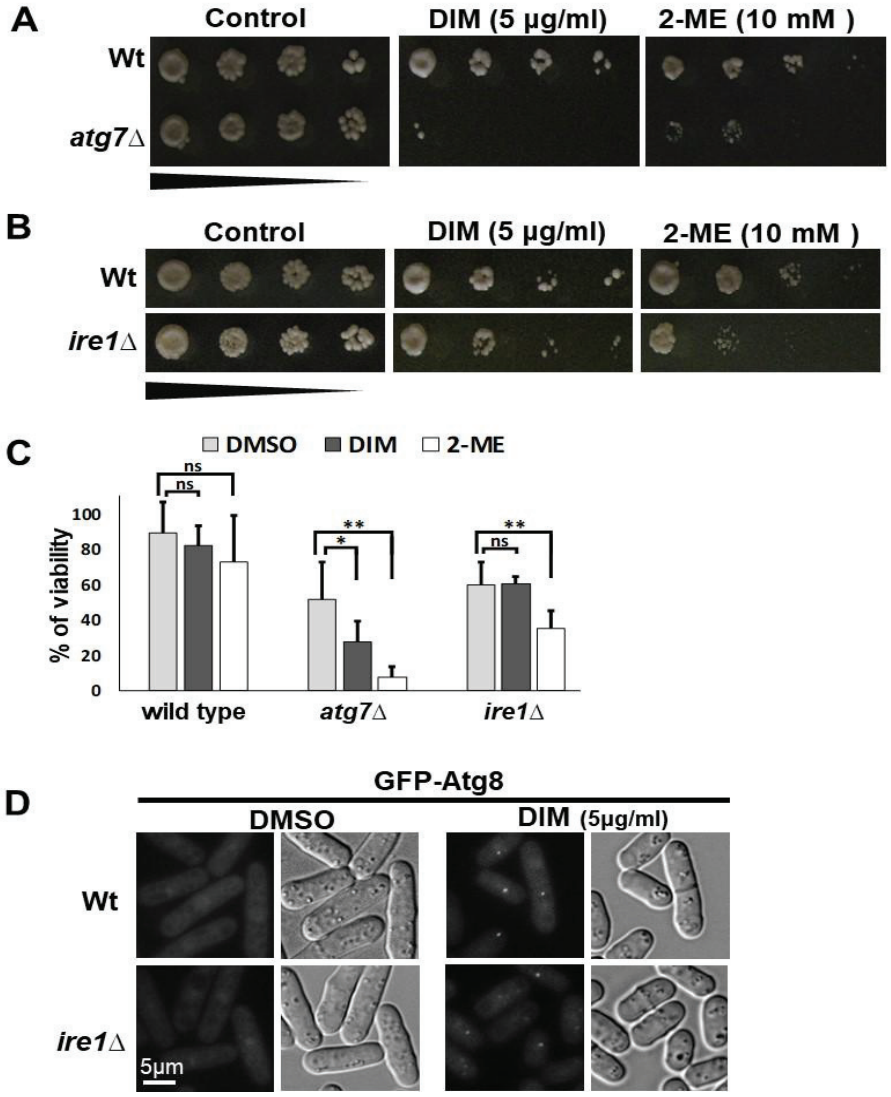

Fig 2.13. Autophagy pathway, but not ER stress response pathway, is required for the resistance to DIM. (A-C) Viability of log-phase cells of wild-type (Wt), *atg7*Δ (A) and *ire1*Δ (B) were studied by spot assay with five-fold serial dilutions in the presence of DIM (5 µg/ml) or 2-ME (10 mM). The images were taken 3-5 days after spotting. The percentages of viability are shown in C. (D) Autophagy induction by DIM (5 µg/ml) was studied in *ire1*Δ mutant expressing GFP-Atg8. The experiment was performed as shown in Fig 2.10. See materials and methods for details.

DIM also induces ER stress and accumulates Ire1, which is responsible for autophagy induction in human ovarian cancer cells [61]. The next question was whether ER stress-response contributes to the viability in the presence of DIM (5 μg/ml) in fission yeast. Ire1 is the major player for ER stress response (UPR regulation) in fission yeast [17, 81], therefore I used *ire1*Δ strain to check its sensitivity to DIM, and asked whether Ire1 pathway involves in cell survival by DIM (5μg/ml) (Figs. 2.13B and C). I found that *ire1*Δ cells were not sensitive to DIM, while they were sensitive to the ER stress condition induced by 2-ME (Figs. 2.13B and C). This data shows that ER stress response does not contribute to survival in the presence of DIM. As mentioned before, DIM induces ER stress in human ovarian cancer cells [61]. The study showed that if mithramycin, ER stress inhibitor, inhibits the ER stress mediated by DIM, therefore ER stress response will be inhibited or not occurred and subsequently, it prevents autophagy induction by DIM. This result suggested that ER stress response is required for autophagy induction by DIM in ovarian cancer cells [61]. I investigated whether ER stress response is required for autophagy induction by DIM in fission yeast. I used *ire1*Δ strain by expressing GFP-Atg8 as an autophagy marker (Fig. 2.13D). I found that GFP-Atg8 foci could still be observed in the *ire1*Δ strain in the presence of DIM (Fig. 2.13D). It means that DIM induces autophagy in *ire1Δ* cells and DIM inducing autophagy may not need ER response to trigger in *ire1Δ* cells.

It is already known that nitrogen starvation [26, 33], sulfur depletion [36], or ER stress [33] induce autophagy in fission yeast. My results suggested that, in contrast to the human case, ER stress response is not required for autophagy induction by a low concentration of DIM (5µg/ml) in fission yeast. It remains unclear how DIM induces autophagy in fission yeast. DIM might mimic nitrogen starvation or sulfur depletion or alternatively, DIM might induce autophagy by an unidentified pathway. Due to my results, the autophagy induction by DIM is Ire1-independent, demonstrating that autophagy induced by DIM is not likely ER stress response-dependent in fission yeast. However, it is unknown if DIM induces ER stress or not. One possibility is that DIM (5µg/ml) does not induce ER stress, therefore, ER stress response is not required to induce autophagy in *ire1Δ* mutant strain. Because if DIM induces ER stress, the viability of *ire1Δ* mutant should be reduced at low DIM concentration (5µg/ml) similar to ER stress condition (2-ME) but it did not.

2.3.7. Nuclear membrane protein, Lem2, is required for the resistance to DIM

I showed that DIM may disrupt NE rapidly (less than 10 min) (Fig. 2.8B), implying that NE could be a direct target or NE disruption might be an early event in the response to DIM. In these cases, the mutant, which has a defect in NM integrity might be more sensitive to DIM. Lem2 is an inner NM protein and plays an important role in regulating NE membrane homeostasis [82] and chromatin

anchoring to the nuclear periphery in fission yeast [83]. I investigated whether *lem2*Δ cells are more sensitive to the low DIM concentration (Fig. 2.14). I found that *lem2*Δ cells are more sensitive at low concentration of DIM (5µg/ml), Therefore, Lem2, is critical for cellular viability in the presence of DIM (Figs. 2.14A and B). I checked the NE morphology in the *lem2*Δ mutant in DIM (5µg/ml) condition (Fig. 2.14C). In contrast to the high concentration of DIM (20 µg/ml) (Fig. 2.8B), the low concentration of DIM (5 µg/ml) did not affect the NE of the wild-type strain (Figs. 2.14C and D and Fig. 2.15). But, NE in the *lem2*Δ mutant was significantly disrupted within four hours of incubation with DIM (5µg/ml). These results confirmed that the NM protein, Lem2, is required for the resistance of NE to DIM.

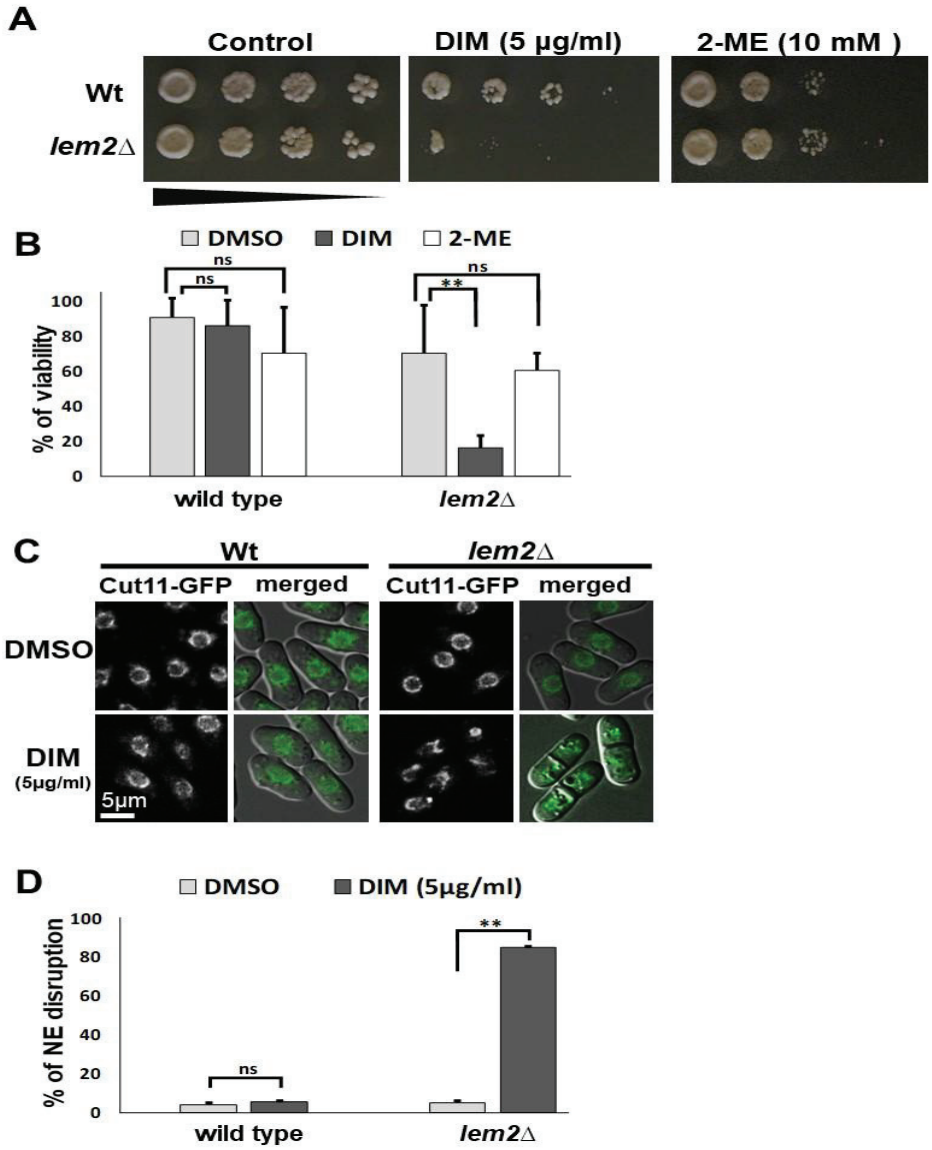

Fig 2.14. Lem2 is required for the resistance to the low concentration of DIM. (A and B) Viability of log-phase cells of wild-type and *lem2*Δ was studied by spot assay with five-fold serial dilutions in the presence of DIM (5 µg/ml) or 2-ME (10 mM). (A) Spotting assay was done as described in Fig. 13A. The percentages of viability are shown in B. (C and D) Fluorescent signals for Cut11-GFP protein in wild-type and *lem2*Δ log-phase cells were seen after four hours incubation with DIM (5 µg/ml) in YEA medium. Images merged with DIC are shown in C. At least 200 cells

were counted with three independent experiments to calculate the percentages of possible NE disruption in wild type and *lem2*Δ are shown in D.

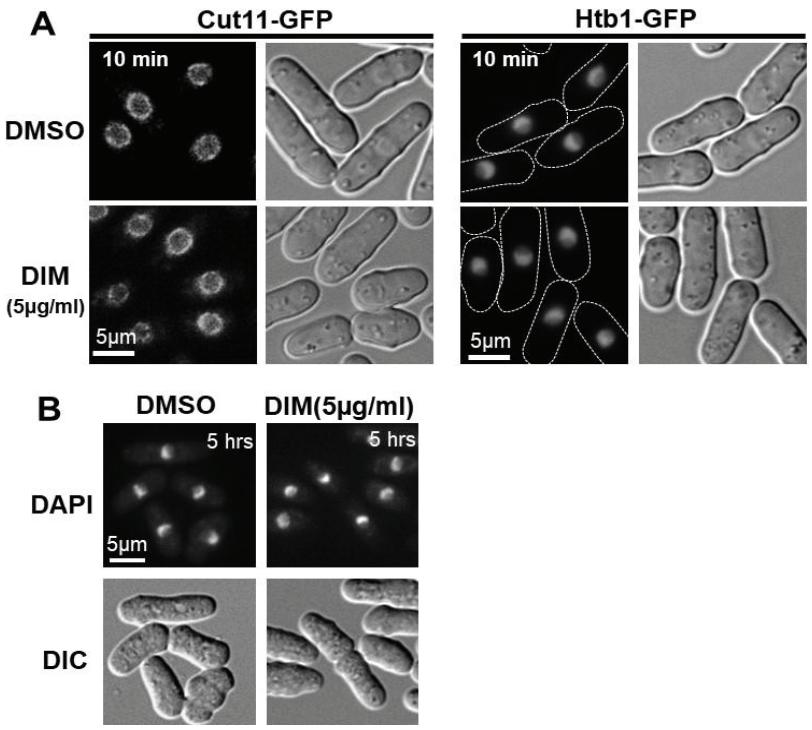

Fig 2.15. DIM does not induce nuclear condensation and fragmentation at a low DIM concentration. (A) DIM (5 µg/ml) was added to the log-phase cells expressing Cut11-GFP and Htb1-GFP and assayed after 10 min incubation (B) DAPI staining was performed for log-phase cells after 5 hours of incubation with DIM (5 µg/ml).

There are some possibilities why the *lem2Δ* cells are more sensitive to the low concentration of DIM. Lem2 acts as a barrier to membrane flow between the NE and other parts of the cellular membrane system [69]. It seems that without Lem2, even a low DIM concentration (5µg/ml) may dramatically affect the membrane flow

between NE and ER membrane which may increase the sensitivity of the *lem2Δ* cells and reduce their viability in the presence of DIM. Another possibility is that, the amount of C24:0 fatty acid, which is important for the survival of yeast cells [84], is reduced in the absence of both Lem2 and Bqt4 (nuclear membrane protein) in fission yeast [67]. It is possible that deletion of *lem2* affects the physical property of the NM including fatty acid composition or possibly membrane protein composition, thus it makes the *lem2Δ* cell more susceptible to the DIM (5µg/ml). The next possibility is related to the potential role of Lem2 protein in the sealing process of NE by ESCRT-III complex (Fig. 2.15). *lem2Δ* cells have defects in the recruitment of proteins such as Vps4 and Cmp7 to NE, therefore, they may have problems in repairing the holes of NE by ESCRT-III [70]. DIM may also make holes in the NE of wild-type cells, which could be repaired (Fig. 2.1). In contrast, in the *lem2*Δ strain with defects in Vps4 expression and Cmp7 localization, ESCRT-III may be unable to seal the NE [70].

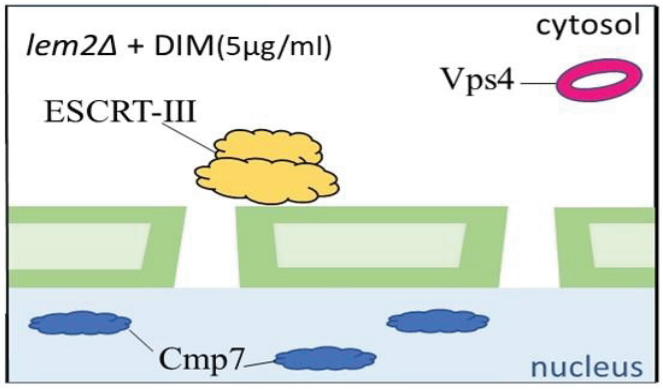

Fig 2.16. NE of *lem2Δ* cells is more sensitive to DIM possibly due to defects in the sealing process. At a low DIM concentration, DIM may induce holes in NE of *lem2Δ* cells however,

without Lem2, cells may have defects in the sealing process because Cmp7 cannot be recruited for ESCRT-III.

2.4. Summary

Here, in chapter 2, I demonstrated that using the DIM in fission yeast shows a dose-dependent behavior that kills the log-phase cells at the high concentration (20µg/ml) and it may cause apoptosis in fission yeast cells (Fig. 2.6). DIM also induces autophagy at a low concentration (5µg/ml) (Fig. 2.10). Apoptosis ad autophagy were new reports about the acute effects of DIM on fission yeast log-phase cells till now. Through the acute assay, I detected that the log-phase cells are more sensitive to DIM than stationary-phase cells (Fig. 2.5) which might be due to the diverse gene transcription or protein compositions in different cell phases. Further, the examination of the nuclear fragmentation, a hallmark of apoptosis, implied the possible apoptosis induction by DIM (20µg/ml) in the log-phase cells (Figs. 2.6C and D). The acute assay showed that 10 min treatment with DIM is enough to trigger the possible apoptosis in log-phase cells (Fig. 2.7B). Evaluation of the morphological events within this 10 min suggested NE disruption and nuclear condensation by DIM (20µg/ml) (Fig. 2.8). It seems the possible NE disruption and subsequent defect in protein transport between the nucleus and the cytoplasm may trigger apoptosis in log-phase cells. To understand if mitochondrial ATPase is the early target of DIM in fission yeast cells, the ATP level was measured in a strain expressing Biosensor Queen [74]. The result revealed that ATP level dropped by

DIM (20µg/ml) after 20 min (Fig. 2.9), while the change and the possible NE disruption by DIM happens within 10 min (Figs. 2.8B and D). This result suggested that NE may be the earlier target of DIM in comparison to mitochondrial ATPase in fission yeast.

My study about the effects of low DIM concentration (5µg/ml) demonstrated autophagy induction in the log-phase cells (Figs. 2.10 and 2.11). I showed that autophagy induction by DIM in fission yeast is an ER stress response-independent pathway (Fig. 2.13 D). Further, I showed that autophagy pathway but not the ER stress response pathway is required to protect the cells at a low DIM concentration (Figs. 2.13 A to C). Moreover, I did not find nuclear condensation, NE disruption and nuclear fragmentation at the low DIM concentration in log-phase cells (Fig. 2.15). I found that NE seems to be intact in wild-type cells when DIM (5µg/ml) is used while in a strain with a defect in NM integrity, *lem2Δ*, the dramatic NE disruption happens (Figs. 2.12C and D). I assumed that the effect of DIM on NE may be the reason for DIM sensitivity in *lem2Δ* cells. This information indicated that besides of autophagy pathway, the status of NE integrity is crucial for maintaining the viability of fission yeast cells at the low DIM concentration. There are some possibilities for the sensitivity of NE in *lem2Δ* in contrast to wild types at DIM (5µg/ml) condition. The potential role of the Lem2 to seal the NE in collaboration with ESCRT-III machinery is one of them. It means that DIM (5µg/ml) may make holes in NE, and in cells without Lem2, Cmp7 cannot be recruited for ESCRT-III

complex [70]. In contrast, in wild-type cells, the holes of NE can be sealed because Lem2 is available to recruit Cmp7. Moreover, Lem2 may be involved in the control of fatty acid metabolism and lipid compositions of NE [67], and DIM may synergistically affect fatty acid metabolism therefore, NE in *lem2Δ* is more sensitive to DIM even at a low concentration. Even, Lem2 acts as a barrier for membrane flow between nucleus and ER [69], and deletion of *lem2* may change the balance of membrane flow and makes the NE more sensitive to the DIM.

Chapter 3

Conclusion

Chapter 3. Conclusion

3.1. Thesis summary

Apoptosis is a process to kill the damaged and unrepairable cells to maintain health in multicellular organisms. Apoptosis is a promising target for cancer therapy because it induces cell death in cancer cells. Autophagy recycles the cellular components and can be induced by stress or nutrient starvation. Autophagy can suppress the growth of cancer cells. Therefore, autophagy induction could be useful in cancer therapy. A study of the drugs that induce apoptosis or autophagy would contribute to developing new anti-cancer drugs. 3,3'-Diindolylmethane (DIM) is one of the promising anti-cancer drugs that can kill the cancer cells trough the apoptosis induction. DIM is a compound derived from the digestion of indole-3-carbinol, found in the broccoli family. DIM induces apoptosis and autophagy in various types of human cancer. DIM has a long-term effect on *Schizosaccharomyces pombe* (*S. pombe*) and extends the lifespan of stationary-phase cells in this type of yeast. *S. pombe* is a species of "fission yeast" which is useful unicellular model to study the mechanism of autophagy and apoptosis. Currently, the mechanisms of DIM to induce apoptosis and autophagy in humans are not fully understood. It is also unknown what acute effects DIM has on log-phase cells in fission yeast. Therefore, in my study a high concentration (20μg/ml) and a low DIM concentration (5μg/ml)

were used to know more about the DIM function in apoptosis and autophagy induction.

I showed that DIM may induce apoptosis and cause autophagy in log-phase cells of fission yeast, which is dose-dependent. Results showed that 10 min treatment with DIM (20µg/ml) is enough to kill log-phase cells and may trigger the apoptosis in cells. My results suggested that 10 min treatment with a high concentration of DIM (20µg/ml) may disrupt the nuclear envelope (NE) structure and induces chromosome condensation dramatically. DIM inhibits mitochondrial ATPase and accumulates in NE of MCF-7 human breast cancer cells. To understand if mitochondrial ATPase is the earlier target of DIM in fission yeast cells or NE, the ATP level was measured in log-phase cells of strain expressing Biosensor Queen at high concentration of DIM (20µg/ml). The result demonstrated that in comparison of NE disruption within 10 min, the ATP level dropped after 20 min. It suggested that NE may be the earlier target of DIM in comparison to mitochondrial ATPase in log-phase cells of fission yeast. The comparison of the DIM-treated stationary and log-phase cells showed that DIM (20µg/ml) does not kill the stationary-phase cells. In fact, DIM cannot induce nuclear condensation or NE disruption or nuclear fragmentation in stationary-phase cells. It may due to the diverse gene transcription or protein compositions in different cell phases.

In contrast to the high DIM concentration, results showed that a low concentration of DIM (5µg/ml) did not disrupt NE structure. I also found that

autophagy induced by DIM (5µg/ml) which is ER stress response independently. It suggested that DIM may mimic nitrogen starvation or sulfur depletion to induce autophagy, or it is possible that unidentified pathway(s) cause(s) autophagy by DIM at low concentration (5µg/ml). I found that an autophagy mutant (*atg7Δ*) is more sensitive to a low concentration of DIM (5µg/ml) than wild-type cells, demonstrating that the autophagy pathway contributes to the survival of cells against DIM. Therefore, autophagy has a protective role to save cells at the low DIM concentration. Moreover, I found that ER stress response pathway is not required for cell survival in exposure to DIM (5µg/ml).

My results demonstrated that the *lem2Δ* mutant is more sensitive to DIM. NE in the *lem2Δ* mutant was disrupted even at the low concentration of DIM (5µg/ml). There are some possibilities for the sensitivity of NE in *lem2*Δ cells to low DIM concentration. It may be due to the change in the fatty acid composition of NE in *lem2Δ* cells. In fission yeast, some fatty acids such as C24:0 fatty acid are required for membrane integrity and cell survival. In the absence of Lem2 and Bqt4 (nuclear membrane protein), some of the required fatty acids for membrane integrity are decreased. It is possible that even in *lem2Δ* single mutant, some of the required fatty acids are reduced, which may make cells more sensitive to DIM (5µg/ml). Due to the effects of DIM on NE of wild-type (20µg/ml), it is also possible that DIM affects fatty acid metabolism. Therefore, DIM may synergistically change the fatty acid composition of NE in *lem2Δ* cells and increase sensitivity of NE to DIM in

these cells. It is known that Lem2 acts as a barrier to membrane flow between the NE and other parts of the cellular membrane system. It seems that without Lem2 as a barrier, even a low DIM concentration may dramatically affect the membrane flow between NE and ER membrane, thus *lem2Δ* cells are sensitive to DIM. Another possibility relates to the potential-role of Lem2 protein in the sealing process of NE by ESCRT-III complex. If it is assumed that in a low concentration, DIM may make holes in NE, the wild-type cells may repair the holes. Hence, NE of wild-type cells seems to be intact at low DIM concentration (5μg/ml), while the cells without Lem2 have defects in the sealing of NE. Thus, *lem2Δ* cells are more sensitive to the low DIM concentration.

Finally, my results demonstrated that the autophagy pathway and NE integrity are important to maintain the viability of log-phase cells in the presence of a low concentration of DIM. The sealing mechanism of NE might be conserved in fission yeast and humans. Further studies about the sealing of NE, when DIM is used, will contribute to the understanding of the direct target(s) of DIM in fission yeast and human. On the other way, comparing the different lipid compositions of NE when DIM is used may help to figure out the mechanism of DIM for NE disruption in fission yeast.

3.2. Achievements of the thesis and more discussion

Here, for the first time, the acute effects of DIM on log-phase cells in fission yeast were studied. DIM had dose-dependent behavior which changes the fate of the log-phase cells. I found that the high concentration of DIM (20µg/ml) kills the log-phase cells which may be caused by apoptosis induction, while the low concentration (5µg/ml) induces autophagy in log-phase cells.

Through the acute assay, I showed that just 10 min treating with DIM (20µg/ml) is enough to trigger the possible apoptosis in log-phase cells. This result gave a hint that the earliest events, which happen within 10 min, may have a role to kill or induce the possible apoptosis in the cells. Further, I found that DIM (20µg/ml) induces remarkable nuclear condensation in log-phase cells after 10 min. I found that NE may be one of the early targets of the DIM in log-phase cells. Time-lapse study demonstrated that NE may be disrupted by DIM (20µg/ml) rapidly within 10 min. Evaluation of NE at low DIM concentration (5µg/ml) showed that DIM causes NE disruption in *lem2Δ* cells, a strain with defects in NM integrity, in contrast to wild-type cells. This result implies that NE integrity is required to resist the low DIM concentration. It also shows that DIM (5µg/ml) may make holes in NE and Lem2 protein may be required to repair the holes, therefore, *lem2Δ* cells are sensitive to the DIM (5µg/ml). Another possibility is that DIM may change the fatty acid composition of NE such as deletion of *lem2*, thus DIM synergistically makes *lem2Δ* cells more sensitive to DIM.

I found that DIM-induced autophagy happens through ER response-independent pathway in fission yeast cells. Spotting assay demonstrated that autophagy protects fission yeast cells at a low DIM concentration (5μg/ml).

It gives a possible hint that why the high concentration of DIM increases the lifespan in fission yeast. It is possible that DIM induces autophagy in a portion of the cells after treatment (20ug/ml). If aging or DIM damages proteins or organelles, the autophagy induced by DIM may recycle them to protect cells and keep them alive. The protective role of DIM induced-autophagy to maintain the viability of the cells is a risky option when DIM is used as an anti-cancer drug. It is possible that even if a high concentration of DIM is used in human cancer cells, some of the cells may uptake a portion of DIM which may cause autophagy in them, not apoptosis. DIM may also extend the lifespan of cancer cells and increase the risk of recurrence, especially when the different effects by DIM were found only by four times change in concentration. If the mechanism of DIM to induce apoptosis and autophagy are conserved, using the fission yeast helps to find the DIM targets in human cells. In this case, the targets of DIM in autophagy and apoptosis-inducing condition should be detected through the chemical genetics approaches. If DIM has different cellular targets at high and low concentrations, the structure of DIM should be changed. To prevent form possible lifespan expansion in cancer cells, the new structure must have only a specific function for apoptosis induction without causing autophagy.

On the other hand, if autophagy induction by DIM is responsible for anti-aging effects, to have an anti-aging drug, the chemical structure of DIM should be changed to have autophagy effects without cell killing effects. In addition, if the earliest target of DIM is NE, therefore, the more efficient structure of DIM should affect the NE only in the cancer cells not the non-cancerous cells.

3.3. Future perspectives

Currently, the earliest target of DIM is not known in fission yeast yet. As mentioned in chapter 1, it was reported that DIM accumulates in nuclear membrane of MCF-7 breast cancer cells after about half an hour [56]. My results also suggested that NE is of the early targets of DIM in fission yeast, and it is possible that DIM directly affects NE. When I compared NE morphology in wild-type and *lem2Δ* strain in low DIM concentration, a possible idea was found which explains DIM may make the holes in NE in both strains. However, DIM-induced holes may be repaired in wild type, thus, NE seems to be intact in wild type. In contrast, NE in *lem2Δ* strains is disrupted, possibly due to the defect in the sealing process. Hence, the investigation of factors involved in the sealing process of NE at low DIM concentration is required to ask if DIM (5µg/ml) makes the holes in NE or not. Cmp7 is recruited for ESCRT-III machinery to seal NE [68]. If the low concentration of DIM (5µg/ml) is used in a strain expressing NE marker and Cmp7

marker, co-localization of both markers and Cmp7 accumulation in NE imply that NE is the target of DIM at both high and low concentrations.

Moreover, another assumption describes that DIM may have synergistic effects on fatty acid metabolism in cells without *lem2*, thus the NE in *lem2Δ* strains is more sensitive to the DIM (5μg/ml). In this case, comparing the different lipid compositions involved in NE at low DIM concentration and no DIM condition may explain the possible mechanism of DIM in NE disruption. It may also help to know how apoptosis is triggered at the early stages, and how the structure of DIM should be improved. Considering that DIM affects NE in fission yeast, this result may make DIM a useful tool for future studies to investigate the factors involved in NE disruption or repairing process.

Appendix

(Protocols and media)

Media Appendix

YEA medium

The complete medium YEA (yeast-extract) was prepared by adding 5 g/l yeast extract (0.5% W/V), 30 g/l glucose (3.0% W/V) and 400 mg/l Adenine (0.4% W/V). Solid media were made by adding the 2% Difco Bacto agar.

EMM medium

The minimal medium EMM (Edinburgh minimal medium) was prepared by adding 10 g/l of glucose (1% W/V), 5 g/l of NH4Cl (0.5% W/V), 4.5 g/l of Na2HPO4. 12H2O (0.45% W/V), 10 ml/l of 100×vitamin solution (1% V/V), 40 ml/l of 25×salt solution (4% V /V), and 10 ml/l of trace elements solution (1% V/V). EMM3 media were supplemented with 50 mg/l leucine, Adenine, or uracil histidine, and lysine when they were essential. To make solid media 2% Difco Bacto agar was added.

PMG (EMMG) medium

To prepare PMG (EMMG) media NH4Cl was replaced by 3.75 g/L of glutamic acid (glutamate). pH:6.0 was adjusted by NaOH(5N) and 20 g/L of glucose was used (2% W/V).

Luria-bertani (LB) medium

Liquid LB medium for *Escherichia coli (E. coli)* was made by adding 10g/l Bacto-tryptone (1% W/V), 5 g/l yeast extract (0.5% W/V), 10 g/l NaCl (1% W/V),

20 µl 5N NaOH (0.02% V/V). Solid LB plates were prepared by adding 2% Difco Bacto agar.

½ YEL medium

To make ½ YEL medium, 43.8g of NaCl (1.5M) and 10g of NaOH (0.5M) were used and dissolved in 500ml of dH_2O.

25×Salt solution

500ml of 25-fold salt solution was made by filtering the solved 37.5g of KH-KH-phthalate, 12.5g of MgCl2 6H2O, 1.25g of Na2SO4, and 0.19g of CaCl2 2H2O in milli-Q water. The final solution was kept at room temperature and used on a laminar airflow to prevent infection.

100×Vitamin solution

100ml of 100-fold vitamin solution was made by filtering the solved 0.1g of Inositol, 0.1g of Nicotinic acid, 0.01g of Ca pantothenate, and 0.01mg of Biotin in milli-Q water. 1mg of the biotin was dissolved in 10ml milli-Q water to make the biotin stock and 1ml of it was used for vitamin solution. The solution was saved at 4^oC and used on a laminar airflow to prevent infection.

10×PBS solution (pH 7.4)

10-fold solution of PBS (pH 7.4) containing NaCl (1.370M), KCl (27mM), Na_2HPO_4 $12H_2O$ (81mM), and KH_2PO_4 (14.7mM) was prepared, filtered, kept in room temperature, and used on a laminar airflow to prevent infection.

100×Trace element solution

500ml of 100-fold trace element solution containing 25mg of H_3BO_3, 20mg of $MnSO_4$ $7H_2O$, 10mg of $FeCl_3$ 6H2O, 8mg of H_2MoO_4 H_2O, 2mg of KI, 2mg of $CuSO_4$ $5H_2O$, 50mg of Citric acid.

NaAC (3M, pH 5.2)

To prepare one litter of NaAC (3M), 408.1 g of sodium acetate (trihydrate) was dissolved in 800 ml H_2O before adjusting the pH (5.2). The final volume was reached to one litter.

Protocol Appendix

DNA extraction

1- Some amount of the desired strains were taken (as much as possible) from YEA plates and suspended in 1.5 ml sterile microtube, containing 100 ml of breaking buffer (2% triton X, 1% SDS, 10mM Tris-HCl (pH 8.0), 10 mM EDTA, and 5mM NaCl).

2- About 200µl of glass beads and 100 µl of phenol/chloroform solution were added to each microtube, and vortexed for 20 sec.

3- The samples were mixed in a microtube for 20 min at 4^{o}C to break cell walls physically (cool room).

4- 100 µl of breaking buffer and 100 µl of phenol/chloroform solution were added to the each sample and vortexed for 100 sec.

5- 200 µl of TE buffer (10 mM Tris-HCl (pH 8.0), 1mM EDTA) was added to the samples and vortexed for 10 sec.

6- Samples were centrifuged for 10 min at 15,000 rpm at 20^{o}C.

7- The upper portions were transferred into the new microtubes. 100 µl of phenol/chloroform solution was added to each sample, vortexed for 10 sec, and centrifuged as explained in step 6.

8- About 250-300 µl of upper portion was transferred to the new tubes for each sample carefully.

9- 300 µl of isopropanol and 30 µl of sodium acetate solution (*NaAC, 3M) were added to the samples and mixed by 20 times shaking (handy). Samples were rested for 5 to 10 min at 20^{o}C.

10- Centrifuge was done similar to the 6th step.

11- Carefully, the liquid portions were discarded. 500 µl of 70 % ethanol (EtOH) was used to wash the precipitated DNA for each sample, then they were centrifuged for 5 min at 15,000 rpm at 20^{o}C.

12- Carefully, ethanol was discarded, and all of the samples were dried by vacuum machine for 3-10 min.

13- 40 µl of sterilized TE was added to every microtube and mixed gently by pipetting and shaking for 1 min, then they were stored at -20^{o}C.

Making agarose gel for electrophoresis

1- At the first step, the desk was covered by plastic wrap, and frames were prepared.

2- To make 400 ml agarose gel, 2 gr of agarose, 398 ml of distilled water, and 8ml of TAE×25* were mixed and microwaved for 5 min or more to dissolve agarose completely (using the appropriate gloves for heat is essential).

3- 400 µl of ethidium bromide (EB) (1mg/ml) was added and mixed with a spoon.

4- The frames were filled with hot agarose solution and the blocked air bubbles were removed then were combs placed.

5- After 3hrs to one overnight, the combs were removed and the gels saved with the frames in a container, containing 1/2×TAE (the same concentration was also used for the tank of electrophoresis apparatus).

*To prepare 25×TAE (pH: 8.0), 14.2 ml of acetic acid and 25 ml of 0.5M EDTA were used. pH amount was adjusted, and finally the total volume increased to 500ml with dH2O.

Polymerase Chain Reaction (PCR)

At the first, PCR program was set and stopped on starting point before preparation of the reactions. A PCR machine (ASTEC PC320) was used. The PCR program was set as below:

- Stage 1 (denaturing): 95ºC for 5 min
- Stage 2 (annealing and extending):

- Step 1: 95ºC for 30 sec
- Step 2: Specific annealing temperature (Tm) for 30 sec
- Step 3: 72º for specific extension time

Repeat stage 2 for 30 times

- Stage 3(final extending): 72ºC for 10 min
- Stage 4: 4ºC till the end

For each sample, 20 µl of PCR mixture was made by mixing 7.5 µl of milli-Q water, 1 µl of forward and reverse primer (10 pM/µl), 0.5 µl of genomic DNA (10 µg/µl) on the ice. Before transferring them to PCR machine, 10 µl of DNA polymerase reaction mixture (premix EX. Taq TM Hot Start Version) was added to each reaction.

Performing the electrophoresis

One µl of PCR product was mixed with 8µl of TE and 1µl of SP mixture. It was loaded for electrophoresis. To prepare SP, at first, a saturated bromophenol blue stock was made by mixing some bromophenol blue and 100 µl of TE in one microtube. SP was made in a new microtube by mixing 20µl of the saturated bromophenol blue and 20µl sucrose (50% g/V).

Ethanol precipitation (purification)

To insert the fragment (PCR fragment or plasmid) into the yeast cells genome, the PCR product /linear plasmid was purified with ethanol precipitation method. Photo was taken from electrophoresis. A comparison of light intensity between DNA marker and fragment gave an assumption about the primary concentration. Briefly, after gathering the primary liquid contains PCR fragment or plasmid, in one sample tube, the total volume was reached to 100 µl by sterile TE. 10 µl of NaAC and 250 µl of absolute ethanol was added and mixed by some

pipetting and inverting. It was stored for 10 min at -20°C and centrifuged for 10 min at 4°C (15,000 rpm). Upper portion was discarded and for ethanol precipitation, without mixing and pipetting, 300 µl of 70% ethanol was used carefully. The centrifuge was repeated for 5 min at 4°C (15,000 rpm). After discarding the ethanol, the plate was dried up with a vacuum machine for 5-10 min. Based on the primary concentration, some amount of sterile TE was added to the plate to have a final concentration (100 ηg/ml).

Direct PCR cloning

In this method, yeast cells will be transformed by desired PCR products which is purified. "*S. pombe* Direct Transformation Kit Wako" (FUJIFILM Wako, Osaka, Japan) was used. 4ml of cell culture in YEA medium was grown to reach 1-1.5×10^7 cells/ml for density. In a new sterilized microtube 100 µl of the transforming reaction, containing 6 µl of DNA or purified PCR product (100 ηg/µl), 4 µl of DNA Carrier and, 90 µl of reaction buffer were mixed. The viscous mixture was mixed with pipetting at least ten times. 3 ml of cell culture was taken and divided between two microtubes (1.5 ml) and precipitated by centrifuge at 5000 rpm for 3 min. Cell pellets were re-suspend by 13µl with YEA medium. The suspended cells were transferred from the first tube to the second tube. 25µl of suspended cell was added into the transforming mixture and vortexed for 10 sec. the mixture was incubate at 37°C for 2 hrs. Cells were precipitated at 5,000 rpm for 1 min and the

plate was suspended in 100 µl sterile water. Cells were dispersed on YEA plates and incubated at 30°C for 24 hrs, followed by replica plating on selective media containing * Kan, Nat or other drugs.

For selection based on nutrients, such as nucleotide or other types of amino acids, after cell precipitation, the cell pellet was suspended with 400 µl ½ YEL liquid medium and incubated for 2 hrs at 30°C. It was precipitated and dispersed on an autotrophic medium plate.

*To prepare the antibiotic stocks of Kan or Nat (100mg/ml), 100mg of G418 sulfate or nourseothricin dihydrogen sulfate was dissolved into 1ml of milli-Q water respectively and filtered. 100 µl of filtered stocked antibiotics was added to 100ml of autoclaved and warm (not hot) YEA, containing agar, to prepare Kan/Nat plates.

Plasmid amplification

To introduce the plasmid to the yeast cells, it was amplified before. Competent cells, Escherichia coli (*E. coli*), were used to increase the plasmid containing the desired gene such as *GFP-atg8* or *nmt4-hmo1*.

LB plate was prepared and 100 µl of ampicillin stock (10 mg/ml) was dispersed completely on LB plate. After drying, competent cells were dispersed on the plates.

To prepare competent cells, 1 µl of purified PCR product (or plasmid) and 15-20 µl of competent cells mixed in a microtube and rested on ice for 5 min and

then were heated at 42ºC for 30 sec. The treated cells were streaked on LB plate containing ampicillin. The reversed plate was incubated overnight at 37ºC to grow the single ampicillin-resistant colonies. Four individual single colonies were taken and separately dissolved in 2 ml of liquid LB, containing 10 µl ampicillin, in sterile glass tubes and incubated overnight (12–16 hours) at 37°C in a shaking incubator. The grown cultures were used for plasmid extraction.

Plasmid extraction

The plasmid was extracted based on quick manufacture protocol for "Wizard Plus SV Minipreps DNA Purification System kit", which is made by "Promega", and available at:

https://www.promega.jp/en/resources/protocols/technical-bulletins/0/wizard-plus-sv-minipreps-dna-purification-system-protocol/

1-10 ml of overnight cultures containing desired plasmid were prepared (12–16 hours at 37°C), and pelleted for 5 min at 15,000 rpm. Remained supernatants were removed completely.

Production of a Cleared Lysate:

1. Pellets were suspended in 250 µl of cell resuspension solution by pipetting.
2. 250 µl of cell lysis solution was added and mixed by inverting the tubes 4 times.
3. 10 µl of alkaline protease solution was added and mixed by inverting the tubes 4 times again and then they were incubated for 5 min at room temperature.

4. 350 µl of neutralization solution was added and mixed by inverting the tubes 4 times.

5. Samples were precipitated by centrifuge for 5 min (15,000 rpm for 10 min at room temperature).

6. The spin columns were inserted into the collection tubes. Total supernatants, the cleared lysates (approximately 850 µl), were decanted into the spin columns.

7. Columns were centrifuged for 1 min at room temperature (15,000 rpm).

8. The collected liquids in collection tubes were discarded and again the spin columns were reinserted into the collection tubes.

9. 750 µl of column wash solution was added to the spin columns, (the solution is a diluted solution with 95% ethanol), and centrifuged for 1 min at room temperature (15,000 rpm).

10. Step 8 was repeated.

11. Step 9 was repeated with 250 µl of column wash solution and the liquids were removed.

12. Drying step was done by centrifuge for 2 min at room temperature and at 15,000rpm speed.

13. The collection tubes were removed and the spin columns inserted into the new sterile 1.5 ml sample tubes and centrifuged for 1 min to be sure about discarding all of the wash solutions.

14. The new sterile sample tube was used and the plasmid was eluted by adding 100 µl of nuclease-free water to the spin column. Centrifuge for 1 min at room temperature and at 15,000rpm speed was done.

15. The spin columns were discarded and sample tubes, containing the plasmids, were stored at -20^{o}C.

16. The plasmid quality was checked by gel electrophoresis.

Plasmid cloning

For plasmid cloning (circular plasmid) same procedure was used such as direct PCR cloning with "*S. pombe* Transformation Kit Wako" (FUJIFILM Wako, Osaka, Japan). 6 µl of plasmid, 4 µl of DNA Carrier and, 90 µl of reaction buffer were mixed to introduce plasmid into the yeast cells. Based on the plasmid marker, the selective media was autotroph to find the colonies containing desired plasmid. Before spreading the cell on a selective medium, the cell pellet was suspended with 400 µl 1/2× liquid YEL medium and incubated for 2 hrs at 30^{o}C. The cells were dispersed on an autotrophic medium plate. In the case of insertion of the linear plasmid into the genome, the digestion step was done before the transforming process. After digestion, 6 µl of linear plasmid was used for transformation.

References

1. Hayles J, Nurse P. Introduction to Fission Yeast as a Model System. Cold Spring Harb Protoc. 2018;2018(5). Epub 2017/07/25. doi: 10.1101/pdb.top079749. PubMed PMID: 28733415.
2. Yanagida M. The model unicellular eukaryote, Schizosaccharomyces pombe. Genome Biol. 2002;3(3):Comment2003. Epub 2002/03/19. doi: 10.1186/gb-2002-3-3-comment2003. PubMed PMID: 11897018; PubMed Central PMCID: PMCPMC139019.
3. Costello G, Rodgers L, Beach D. Fission yeast enters the stationary phase G0 state from either mitotic G1 or G2. Current Genetics. 1986;11(2):119-25. doi: 10.1007/BF00378203.
4. Ding R, West RR, Morphew DM, Oakley BR, McIntosh JR. The spindle pole body of Schizosaccharomyces pombe enters and leaves the nuclear envelope as the cell cycle proceeds. Mol Biol Cell. 1997;8(8):1461-79. Epub 1997/08/01. doi: 10.1091/mbc.8.8.1461. PubMed PMID: 9285819; PubMed Central PMCID: PMCPMC276170.
5. Olsson I, Bjerling P. Advancing our understanding of functional genome organisation through studies in the fission yeast. Curr Genet. 2011;57(1):1-12. Epub 2010/11/30. doi: 10.1007/s00294-010-0327-x. PubMed PMID: 21113595; PubMed Central PMCID: PMCPMC3023017.
6. Vyas A, Freitas AV, Ralston ZA, Tang Z. Fission Yeast Schizosaccharomyces pombe: A Unicellular "Micromammal" Model Organism. Curr Protoc. 2021;1(6):e151. Epub 2021/06/09. doi: 10.1002/cpz1.151. PubMed PMID: 34101381; PubMed Central PMCID: PMCPMC8193909.

7. Agus HH, Kok G, Derinoz E, Oncel D, Yilmaz S. Involvement of Pca1 in ROS-mediated apoptotic cell death induced by alpha-thujone in the fission yeast (Schizosaccharomyces pombe). FEMS Yeast Res. 2020;20(4). Epub 2020/04/30. doi: 10.1093/femsyr/foaa022. PubMed PMID: 32347926.
8. Fröhlich KU, Fussi H, Ruckenstuhl C. Yeast apoptosis--from genes to pathways. Semin Cancer Biol. 2007;17(2):112-21. Epub 2007/01/09. doi: 10.1016/j.semcancer.2006.11.006. PubMed PMID: 17207637.
9. Lin SJ, Austriaco N. Aging and cell death in the other yeasts, Schizosaccharomyces pombe and Candida albicans. FEMS Yeast Res. 2014;14(1):119-35. Epub 2013/11/12. doi: 10.1111/1567-1364.12113. PubMed PMID: 24205865; PubMed Central PMCID: PMCPMC4000287.
10. Mutoh N, Kitajima S, Ichihara S. Apoptotic cell death in the fission yeast Schizosaccharomyces pombe induced by valproic acid and its extreme susceptibility to pH change. Biosci Biotechnol Biochem. 2011;75(6):1113-8. Epub 2011/06/15. doi: 10.1271/bbb.110019. PubMed PMID: 21670521.
11. Kohda TA, Tanaka K, Konomi M, Sato M, Osumi M, Yamamoto M. Fission yeast autophagy induced by nitrogen starvation generates a nitrogen source that drives adaptation processes. Genes Cells. 2007;12(2):155-70. Epub 2007/02/14. doi: 10.1111/j.1365-2443.2007.01041.x. PubMed PMID: 17295836.
12. Mukaiyama H, Nakase M, Nakamura T, Kakinuma Y, Takegawa K. Autophagy in the fission yeast Schizosaccharomyces pombe. FEBS Lett. 2010;584(7):1327-34. Epub 2009/12/29. doi: 10.1016/j.febslet.2009.12.037. PubMed PMID: 20036658.
13. Rodriguez-Menocal L, D'Urso G. Programmed cell death in fission yeast. FEMS Yeast Res. 2004;5(2):111-7. Epub 2004/10/19. doi: 10.1016/j.femsyr.2004.07.007. PubMed PMID: 15489193.

14. Agus HH, Sarp C, Cemiloglu M. Oxidative stress and mitochondrial impairment mediated apoptotic cell death induced by terpinolene in Schizosaccharomyces pombe. Toxicol Res (Camb). 2018;7(5):848-58. Epub 2018/10/13. doi: 10.1039/c8tx00100f. PubMed PMID: 30310662; PubMed Central PMCID: PMCPMC6116180.
15. Guérin R, Beauregard PB, Leroux A, Rokeach LA. Calnexin regulates apoptosis induced by inositol starvation in fission yeast. PLoS One. 2009;4(7):e6244. Epub 2009/07/17. doi: 10.1371/journal.pone.0006244. PubMed PMID: 19606215; PubMed Central PMCID: PMCPMC2705804.
16. Low CP, Liew LP, Pervaiz S, Yang H. Apoptosis and lipoapoptosis in the fission yeast Schizosaccharomyces pombe. FEMS Yeast Res. 2005;5(12):1199-206. Epub 2005/09/03. doi: 10.1016/j.femsyr.2005.07.004. PubMed PMID: 16137929.
17. Guérin R, Arseneault G, Dumont S, Rokeach LA. Calnexin is involved in apoptosis induced by endoplasmic reticulum stress in the fission yeast. Mol Biol Cell. 2008;19(10):4404-20. Epub 2008/08/15. doi: 10.1091/mbc.e08-02-0188. PubMed PMID: 18701708; PubMed Central PMCID: PMCPMC2555920.
18. Agus HH, Sengoz CO, Yilmaz S. Oxidative stress-mediated apoptotic cell death induced by camphor in sod1-deficient Schizosaccharomyces pombe. Toxicol Res (Camb). 2019;8(2):216-26. Epub 2019/04/02. doi: 10.1039/c8tx00279g. PubMed PMID: 30931102; PubMed Central PMCID: PMCPMC6404167.
19. Low CP, Shui G, Liew LP, Buttner S, Madeo F, Dawes IW, et al. Caspase-dependent and -independent lipotoxic cell-death pathways in fission yeast. J Cell Sci. 2008;121(Pt 16):2671-84. Epub 2008/07/26. doi: 10.1242/jcs.028977. PubMed PMID: 18653539.

20. Zhang Q, Chieu HK, Low CP, Zhang S, Heng CK, Yang H. Schizosaccharomyces pombe cells deficient in triacylglycerols synthesis undergo apoptosis upon entry into the stationary phase. J Biol Chem. 2003;278(47):47145-55. Epub 2003/09/10. doi: 10.1074/jbc.M306998200. PubMed PMID: 12963726.
21. Jürgensmeier JM, Krajewski S, Armstrong RC, Wilson GM, Oltersdorf T, Fritz LC, et al. Bax- and Bak-induced cell death in the fission yeast Schizosaccharomyces pombe. Mol Biol Cell. 1997;8(2):325-39. Epub 1997/02/01. doi: 10.1091/mbc.8.2.325. PubMed PMID: 9190211; PubMed Central PMCID: PMCPMC276083.
22. Youle RJ, Strasser A. The BCL-2 protein family: opposing activities that mediate cell death. Nat Rev Mol Cell Biol. 2008;9(1):47-59. Epub 2007/12/22. doi: 10.1038/nrm2308. PubMed PMID: 18097445.
23. Oda K, Kawasaki N, Fukuyama M, Ikeda S. Ectopic expression of mitochondria endonuclease Pnu1p from Schizosaccharomyces pombe induces cell death of the yeast. J Biochem Mol Biol. 2007;40(6):1095-9. Epub 2007/12/01. doi: 10.5483/bmbrep.2007.40.6.1095. PubMed PMID: 18047809.
24. Vessoni AT, Filippi-Chiela EC, Menck CF, Lenz G. Autophagy and genomic integrity. Cell Death Differ. 2013;20(11):1444-54. Epub 2013/08/13. doi: 10.1038/cdd.2013.103. PubMed PMID: 23933813; PubMed Central PMCID: PMCPMC3792426.
25. Yun CW, Lee SH. The Roles of Autophagy in Cancer. Int J Mol Sci. 2018;19(11). Epub 2018/11/08. doi: 10.3390/ijms19113466. PubMed PMID: 30400561; PubMed Central PMCID: PMCPMC6274804.
26. Mukaiyama H, Kajiwara S, Hosomi A, Giga-Hama Y, Tanaka N, Nakamura T, et al. Autophagy-deficient Schizosaccharomyces pombe mutants undergo partial sporulation during nitrogen starvation. Microbiology (Reading).

2009;155(Pt 12):3816-26. Epub 2009/09/26. doi: 10.1099/mic.0.034389-0. PubMed PMID: 19778961.

27. Xu DD, Du LL. Fission Yeast Autophagy Machinery. Cells. 2022;11(7). Epub 2022/04/13. doi: 10.3390/cells11071086. PubMed PMID: 35406650; PubMed Central PMCID: PMCPMC8997447.
28. Zaffagnini G, Martens S. Mechanisms of Selective Autophagy. J Mol Biol. 2016;428(9 Pt A):1714-24. Epub 2016/02/16. doi: 10.1016/j.jmb.2016.02.004. PubMed PMID: 26876603; PubMed Central PMCID: PMCPMC4871809.
29. Yu ZQ, Sun LL, Jiang ZD, Liu XM, Zhao D, Wang HT, et al. Atg38-Atg8 interaction in fission yeast establishes a positive feedback loop to promote autophagy. Autophagy. 2020;16(11):2036-51. Epub 2020/01/17. doi: 10.1080/15548627.2020.1713644. PubMed PMID: 31941401; PubMed Central PMCID: PMCPMC7595586.
30. Sun LL, Li M, Suo F, Liu XM, Shen EZ, Yang B, et al. Global analysis of fission yeast mating genes reveals new autophagy factors. PLoS Genet. 2013;9(8):e1003715. Epub 2013/08/21. doi: 10.1371/journal.pgen.1003715. PubMed PMID: 23950735; PubMed Central PMCID: PMCPMC3738441.
31. Sun J, Shigemi H, Cao M, Qin E, Tang J, Shen J, et al. Minocycline Induces Autophagy and Inhibits Cell Proliferation in LPS-Stimulated THP-1 Cells. Biomed Res Int. 2020;2020:5459209. Epub 2020/08/09. doi: 10.1155/2020/5459209. PubMed PMID: 32766308; PubMed Central PMCID: PMCPMC7387962.
32. Mizushima N, Yoshimori T, Ohsumi Y. The role of Atg proteins in autophagosome formation. Annu Rev Cell Dev Biol. 2011;27:107-32. Epub 2011/08/02. doi: 10.1146/annurev-cellbio-092910-154005. PubMed PMID: 21801009.
33. Zhao D, Zou CX, Liu XM, Jiang ZD, Yu ZQ, Suo F, et al. A UPR-Induced Soluble ER-Phagy Receptor Acts with VAPs to Confer ER Stress Resistance.

Mol Cell. 2020;79(6):963-77.e3. Epub 2020/08/01. doi: 10.1016/j.molcel.2020.07.019. PubMed PMID: 32735772.

34. Matsuhara H, Yamamoto A. Autophagy is required for efficient meiosis progression and proper meiotic chromosome segregation in fission yeast. Genes Cells. 2016;21(1):65-87. Epub 2015/12/24. doi: 10.1111/gtc.12320. PubMed PMID: 26696398.

35. Núñez A, Dulude D, Jbel M, Rokeach LA. Calnexin is essential for survival under nitrogen starvation and stationary phase in Schizosaccharomyces pombe. PLoS One. 2015;10(3):e0121059. Epub 2015/03/25. doi: 10.1371/journal.pone.0121059. PubMed PMID: 25803873; PubMed Central PMCID: PMCPMC4372366.

36. Shimasaki T, Okamoto K, Ohtsuka H, Aiba H. Sulfur depletion induces autophagy through Ecl1 family genes in fission yeast. Genes Cells. 2020;25(12):825-30. Epub 2020/10/17. doi: 10.1111/gtc.12815. PubMed PMID: 33064910.

37. Otsubo Y, Nakashima A, Yamamoto M, Yamashita A. TORC1-Dependent Phosphorylation Targets in Fission Yeast. Biomolecules. 2017;7(3). Epub 2017/07/04. doi: 10.3390/biom7030050. PubMed PMID: 28671615; PubMed Central PMCID: PMCPMC5618231.

38. Verhoeven DT, Verhagen H, Goldbohm RA, van den Brandt PA, van Poppel G. A review of mechanisms underlying anticarcinogenicity by brassica vegetables. Chem Biol Interact. 1997;103(2):79-129. Epub 1997/02/28. doi: 10.1016/s0009-2797(96)03745-3. PubMed PMID: 9055870.

39. Lanza-Jacoby S, Cheng G. 3,3'-Diindolylmethane enhances apoptosis in docetaxel-treated breast cancer cells by generation of reactive oxygen species. Pharm Biol. 2018;56(1):407-14. Epub 2018/10/12. doi: 10.1080/13880209.2018.1495747. PubMed PMID: 30301388; PubMed Central PMCID: PMCPMC6179060.

40. Wang Z, Yu BW, Rahman KM, Ahmad F, Sarkar FH. Induction of growth arrest and apoptosis in human breast cancer cells by 3,3-diindolylmethane is associated with induction and nuclear localization of p27kip. Mol Cancer Ther. 2008;7(2):341-9. Epub 2008/02/19. doi: 10.1158/1535-7163.Mct-07-0476. PubMed PMID: 18281517.
41. Cheng JS, Shu SS, Kuo CC, Chou CT, Tsai WL, Fang YC, et al. Effect of diindolylmethane on Ca(2+) movement and viability in HA59T human hepatoma cells. Arch Toxicol. 2011;85(10):1257-66. Epub 2011/03/17. doi: 10.1007/s00204-011-0670-9. PubMed PMID: 21409406.
42. Munakarmi S, Shrestha J, Shin HB, Lee GH, Jeong YJ. 3,3'-Diindolylmethane Suppresses the Growth of Hepatocellular Carcinoma by Regulating Its Invasion, Migration, and ER Stress-Mediated Mitochondrial Apoptosis. Cells. 2021;10(5). Epub 2021/06/03. doi: 10.3390/cells10051178. PubMed PMID: 34066056; PubMed Central PMCID: PMCPMC8151225.
43. Nachshon-Kedmi M, Yannai S, Haj A, Fares FA. Indole-3-carbinol and 3,3'-diindolylmethane induce apoptosis in human prostate cancer cells. Food Chem Toxicol. 2003;41(6):745-52. Epub 2003/05/10. doi: 10.1016/s0278-6915(03)00004-8. PubMed PMID: 12738179.
44. Tsai JY, Chou CT, Liu SI, Liang WZ, Kuo CC, Liao WC, et al. Effect of diindolylmethane on Ca2+ homeostasis and viability in PC3 human prostate cancer cells. J Recept Signal Transduct Res. 2012;32(5):271-8. Epub 2012/08/01. doi: 10.3109/10799893.2012.707212. PubMed PMID: 22845469.
45. Gao X, Liu J, Cho KB, Kedika S, Guo B. Chemopreventive Agent 3,3'-Diindolylmethane Inhibits MDM2 in Colorectal Cancer Cells. Int J Mol Sci. 2020;21(13). Epub 2020/07/08. doi: 10.3390/ijms21134642. PubMed PMID: 32629830; PubMed Central PMCID: PMCPMC7370074.
46. Kim EJ, Park SY, Shin HK, Kwon DY, Surh YJ, Park JH. Activation of caspase-8 contributes to 3,3'-Diindolylmethane-induced apoptosis in colon

cancer cells. J Nutr. 2007;137(1):31-6. Epub 2006/12/22. doi: 10.1093/jn/137.1.31. PubMed PMID: 17182797.

47. Tian X, Liu K, Zu X, Ma F, Li Z, Lee M, et al. 3,3'-Diindolylmethane inhibits patient-derived xenograft colon tumor growth by targeting COX1/2 and ERK1/2. Cancer Lett. 2019;448:20-30. Epub 2019/02/05. doi: 10.1016/j.canlet.2019.01.031. PubMed PMID: 30716361.

48. Ge X, Yannai S, Rennert G, Gruener N, Fares FA. 3,3'-Diindolylmethane induces apoptosis in human cancer cells. Biochem Biophys Res Commun. 1996;228(1):153-8. Epub 1996/11/01. doi: 10.1006/bbrc.1996.1631. PubMed PMID: 8912651.

49. Nachshon-Kedmi M, Yannai S, Fares FA. Induction of apoptosis in human prostate cancer cell line, PC3, by 3,3'-diindolylmethane through the mitochondrial pathway. Br J Cancer. 2004;91(7):1358-63. Epub 2004/08/26. doi: 10.1038/sj.bjc.6602145. PubMed PMID: 15328526; PubMed Central PMCID: PMCPMC2409910.

50. Savino JA, 3rd, Evans JF, Rabinowitz D, Auborn KJ, Carter TH. Multiple, disparate roles for calcium signaling in apoptosis of human prostate and cervical cancer cells exposed to diindolylmethane. Mol Cancer Ther. 2006;5(3):556-63. Epub 2006/03/21. doi: 10.1158/1535-7163.Mct-05-0355. PubMed PMID: 16546969.

51. Ye Y, Ye F, Li X, Yang Q, Zhou J, Xu W, et al. 3,3'-diindolylmethane exerts antiproliferation and apoptosis induction by TRAF2-p38 axis in gastric cancer. Anticancer Drugs. 2021;32(2):189-202. Epub 2020/12/15. doi: 10.1097/cad.0000000000000997. PubMed PMID: 33315588; PubMed Central PMCID: PMCPMC7790923.

52. Liang K, Qian WH, Zong J. 3,3'‐Diindolylmethane attenuates cardiomyocyte hypoxia by modulating autophagy in H9c2 cells. Mol Med Rep.

2017;16(6):9553-60. Epub 2017/10/19. doi: 10.3892/mmr.2017.7788. PubMed PMID: 29039568.

53. Lee BD, Yoo JM, Baek SY, Li FY, Sok DE, Kim MR. 3,3'-Diindolylmethane Promotes BDNF and Antioxidant Enzyme Formation via TrkB/Akt Pathway Activation for Neuroprotection against Oxidative Stress-Induced Apoptosis in Hippocampal Neuronal Cells. Antioxidants (Basel). 2019;9(1). Epub 2019/12/22. doi: 10.3390/antiox9010003. PubMed PMID: 31861353; PubMed Central PMCID: PMCPMC7023184.

54. Riby JE, Firestone GL, Bjeldanes LF. 3,3'-diindolylmethane reduces levels of HIF-1alpha and HIF-1 activity in hypoxic cultured human cancer cells. Biochem Pharmacol. 2008;75(9):1858-67. Epub 2008/03/11. doi: 10.1016/j.bcp.2008.01.017. PubMed PMID: 18329003; PubMed Central PMCID: PMCPMC2387239.

55. Gong Y, Sohn H, Xue L, Firestone GL, Bjeldanes LF. 3,3'-Diindolylmethane is a novel mitochondrial H(+)-ATP synthase inhibitor that can induce p21(Cip1/Waf1) expression by induction of oxidative stress in human breast cancer cells. Cancer Res. 2006;66(9):4880-7. Epub 2006/05/03. doi: 10.1158/0008-5472.Can-05-4162. PubMed PMID: 16651444.

56. Staub RE, Onisko B, Bjeldanes LF. Fate of 3,3'-diindolylmethane in cultured MCF-7 human breast cancer cells. Chem Res Toxicol. 2006;19(3):436-42. Epub 2006/03/21. doi: 10.1021/tx050325z. PubMed PMID: 16544949.

57. Nakamura S, Yoshimori T. Autophagy and Longevity. Mol Cells. 2018;41(1):65-72. Epub 2018/01/27. doi: 10.14348/molcells.2018.2333. PubMed PMID: 29370695; PubMed Central PMCID: PMCPMC5792715.

58. Azzopardi M, Farrugia G, Balzan R. Cell-cycle involvement in autophagy and apoptosis in yeast. Mech Ageing Dev. 2017;161(Pt B):211-24. Epub 2016/07/28. doi: 10.1016/j.mad.2016.07.006. PubMed PMID: 27450768.

59. Chavez-Dominguez R, Perez-Medina M, Lopez-Gonzalez JS, Galicia-Velasco M, Aguilar-Cazares D. The Double-Edge Sword of Autophagy in Cancer: From Tumor Suppression to Pro-tumor Activity. Front Oncol. 2020;10:578418. Epub 2020/10/30. doi: 10.3389/fonc.2020.578418. PubMed PMID: 33117715; PubMed Central PMCID: PMCPMC7575731.
60. Jung S, Jeong H, Yu S-W. Autophagy as a decisive process for cell death. Experimental & Molecular Medicine. 2020;52(6):921-30. doi: 10.1038/s12276-020-0455-4.
61. Kandala PK, Srivastava SK. Regulation of macroautophagy in ovarian cancer cells in vitro and in vivo by controlling glucose regulatory protein 78 and AMPK. Oncotarget. 2012;3(4):435-49. Epub 2012/05/09. doi: 10.18632/oncotarget.483. PubMed PMID: 22564965; PubMed Central PMCID: PMCPMC3380578.
62. Pan Z, Xie Y, Bai J, Lin Q, Cui X, Zhang N. Bufalin suppresses colorectal cancer cell growth through promoting autophagy in vivo and in vitro. RSC Advances. 2018;8(68):38910-8. doi: 10.1039/C8RA06566G.
63. Ye Y, Fang Y, Xu W, Wang Q, Zhou J, Lu R. 3,3'-Diindolylmethane induces anti-human gastric cancer cells by the miR-30e-ATG5 modulating autophagy. Biochem Pharmacol. 2016;115:77-84. Epub 2016/07/04. doi: 10.1016/j.bcp.2016.06.018. PubMed PMID: 27372603.
64. Goldberg AA, Draz H, Montes-Grajales D, Olivero-Verbél J, Safe SH, Sanderson JT. 3,3'-Diindolylmethane (DIM) and its ring-substituted halogenated analogs (ring-DIMs) induce differential mechanisms of survival and death in androgen-dependent and -independent prostate cancer cells. Genes Cancer. 2015;6(5-6):265-80. Epub 2015/07/01. doi: 10.18632/genesandcancer.98. PubMed PMID: 26124925; PubMed Central PMCID: PMCPMC4482247.

65. Rzemieniec J, Wnuk A, Lasoń W, Bilecki W, Kajta M. The neuroprotective action of 3,3′-diindolylmethane against ischemia involves an inhibition of apoptosis and autophagy that depends on HDAC and AhR/CYP1A1 but not ERα/CYP19A1 signaling. Apoptosis. 2019;24(5):435-52. doi: 10.1007/s10495-019-01522-2.
66. Hirano Y, Asakawa H, Sakuno T, Haraguchi T, Hiraoka Y. Nuclear Envelope Proteins Modulating the Heterochromatin Formation and Functions in Fission Yeast. Cells. 2020;9(8). Epub 2020/08/23. doi: 10.3390/cells9081908. PubMed PMID: 32824370; PubMed Central PMCID: PMCPMC7464478.
67. Kinugasa Y, Hirano Y, Sawai M, Ohno Y, Shindo T, Asakawa H, et al. The very-long-chain fatty acid elongase Elo2 rescues lethal defects associated with loss of the nuclear barrier function in fission yeast cells. J Cell Sci. 2019;132(10). Epub 2019/04/13. doi: 10.1242/jcs.229021. PubMed PMID: 30975915.
68. Gu M, LaJoie D, Chen OS, von Appen A, Ladinsky MS, Redd MJ, et al. LEM2 recruits CHMP7 for ESCRT-mediated nuclear envelope closure in fission yeast and human cells. Proc Natl Acad Sci U S A. 2017;114(11):E2166-e75. Epub 2017/03/01. doi: 10.1073/pnas.1613916114. PubMed PMID: 28242692; PubMed Central PMCID: PMCPMC5358359.
69. Kume K, Cantwell H, Burrell A, Nurse P. Nuclear membrane protein Lem2 regulates nuclear size through membrane flow. Nat Commun. 2019;10(1):1871. Epub 2019/04/25. doi: 10.1038/s41467-019-09623-x. PubMed PMID: 31015410; PubMed Central PMCID: PMCPMC6478680.
70. Hirano Y, Kinugasa Y, Osakada H, Shindo T, Kubota Y, Shibata S, et al. Lem2 and Lnp1 maintain the membrane boundary between the nuclear envelope and endoplasmic reticulum. Commun Biol. 2020;3(1):276. Epub 2020/06/03. doi: 10.1038/s42003-020-0999-9. PubMed PMID: 32483293; PubMed Central PMCID: PMCPMC7264229.

71. Lusk CP, Ader NR. CHMPions of repair: Emerging perspectives on sensing and repairing the nuclear envelope barrier. Curr Opin Cell Biol. 2020;64:25-33. Epub 2020/02/28. doi: 10.1016/j.ceb.2020.01.011. PubMed PMID: 32105978; PubMed Central PMCID: PMCPMC7371540.
72. Stephan J, Franke J, Ehrenhofer-Murray AE. Chemical genetic screen in fission yeast reveals roles for vacuolar acidification, mitochondrial fission, and cellular GMP levels in lifespan extension. Aging Cell. 2013;12(4):574-83. Epub 2013/03/26. doi: 10.1111/acel.12077. PubMed PMID: 23521895.
73. Kimmig P, Diaz M, Zheng J, Williams CC, Lang A, Aragón T, et al. The unfolded protein response in fission yeast modulates stability of select mRNAs to maintain protein homeostasis. Elife. 2012;1:e00048. Epub 2012/10/16. doi: 10.7554/eLife.00048. PubMed PMID: 23066505; PubMed Central PMCID: PMCPMC3470409.
74. Ito H, Sugawara T, Shinkai S, Mizukawa S, Kondo A, Senda H, et al. Spindle pole body movement is affected by glucose and ammonium chloride in fission yeast. Biochem Biophys Res Commun. 2019;511(4):820-5. Epub 2019/03/09. doi: 10.1016/j.bbrc.2019.02.128. PubMed PMID: 30846209.
75. Takaine M, Ueno M, Kitamura K, Imamura H, Yoshida S. Reliable imaging of ATP in living budding and fission yeast. J Cell Sci. 2019;132(8). Epub 2019/03/13. doi: 10.1242/jcs.230649. PubMed PMID: 30858198.
76. Kim SM. Cellular and Molecular Mechanisms of 3,3'-Diindolylmethane in Gastrointestinal Cancer. Int J Mol Sci. 2016;17(7). Epub 2016/07/23. doi: 10.3390/ijms17071155. PubMed PMID: 27447608; PubMed Central PMCID: PMCPMC4964527.
77. Taricani L, Tejada ML, Young PG. The fission yeast ES2 homologue, Bis1, interacts with the Ish1 stress-responsive nuclear envelope protein. J Biol Chem. 2002;277(12):10562-72. Epub 2001/12/26. doi: 10.1074/jbc.M110686200. PubMed PMID: 11751918.

78. Higby KJ, Bischak MM, Campbell CA, Anderson RG, Broskin SA, Foltz LE, et al. 5-Flurouracil disrupts nuclear export and nuclear pore permeability in a calcium dependent manner. Apoptosis. 2017;22(3):393-405. Epub 2016/12/22. doi: 10.1007/s10495-016-1338-y. PubMed PMID: 28000054.
79. Muneyuki E, Makino M, Kamata H, Kagawa Y, Yoshida M, Hirata H. Inhibitory effect of NaN3 on the F0F1 ATPase of submitochondrial particles as related to nucleotide binding. Biochim Biophys Acta. 1993;1144(1):62-8. Epub 1993/08/16. doi: 10.1016/0005-2728(93)90031-a. PubMed PMID: 8347662.
80. Fukuda T, Ebi Y, Saigusa T, Furukawa K, Yamashita SI, Inoue K, et al. Atg43 tethers isolation membranes to mitochondria to promote starvation-induced mitophagy in fission yeast. Elife. 2020;9. Epub 2020/11/04. doi: 10.7554/eLife.61245. PubMed PMID: 33138913; PubMed Central PMCID: PMCPMC7609059.
81. Hernández-Elvira M, Torres-Quiroz F, Escamilla-Ayala A, Domínguez-Martin E, Escalante R, Kawasaki L, et al. The Unfolded Protein Response Pathway in the Yeast Kluyveromyces lactis. A Comparative View among Yeast Species. Cells. 2018;7(8). Epub 2018/08/17. doi: 10.3390/cells7080106. PubMed PMID: 30110882; PubMed Central PMCID: PMCPMC6116095.
82. Yang HJ, Iwamoto M, Hiraoka Y, Haraguchi T. Function of nuclear membrane proteins in shaping the nuclear envelope integrity during closed mitosis. J Biochem. 2017;161(6):471-7. Epub 2017/04/12. doi: 10.1093/jb/mvx020. PubMed PMID: 28398483.
83. Gonzalez Y, Saito A, Sazer S. Fission yeast Lem2 and Man1 perform fundamental functions of the animal cell nuclear lamina. Nucleus. 2012;3(1):60-76. Epub 2012/04/28. doi: 10.4161/nucl.18824. PubMed PMID: 22540024; PubMed Central PMCID: PMCPMC3337167.

84. Cerantola V, Vionnet C, Aebischer OF, Jenny T, Knudsen J, Conzelmann A. Yeast sphingolipids do not need to contain very long chain fatty acids. Biochem J. 2007;401(1):205-16. Epub 2006/09/22. doi: 10.1042/bj20061128. PubMed PMID: 16987101; PubMed Central PMCID: PMCPMC1698682.

Acknowledgment

First, I would like to be grateful to Dr. Masaru Ueno, my dear supervisor, for his patience, kindness, motivation, and valuable comments to improve my writing of this thesis. He learned me to improve my abilities as a beginner researcher. It was my honor to have a chance to be trained by him. I thanks to my reviewer committee, Professor Takashi Toda, Dr. Takahiro Chihara, Dr. Masaki Mizunuma and Dr. Takuya Imamura for their revision of my thesis.

I am grateful to Dr. Mitsuhiro Yanagida, Dr. Atsushi Matsuda, Dr. Yasushi Hiraoka, Dr. Peter Walter, Dr. Ayumu Yamamoto, Dr. Yoshinori Watanabe, and Dr. Takeshi Sakuno, Dr. A. Francis Stewart, Dr. Li-Lin Du and Sayaka Suzuki for the strains and plasmids, respectively. I am also thankful to Dr. Hizlan Hincal Agus for his helpful guidance. I am also grateful to the Ministry of Education, Culture, Sports, Science and Technology (MEXT) for providing me scholarship to live and educate in Japan.

I proud to have my kind friends and lab members that they collaborated and helped me a lot. Thanks for creating the beautiful and friendly moments for me. Finally, my sincere thanks are to my lovely family, even though they are far from thousand kilometers; my dear parents, my kind sister, my brother, and his nice family.